

CZECH TECHNICAL UNIVERSITY IN  
PRAGUE  
Faculty of Civil Engineering



DIPLOMA THESIS

Pre-stressed building of the National Technical  
Library in Prague

Fiorella Silvana Salcedo Salinas

Supervisor: doc. Ing. Marek Foglar, PhD

Prague, May 2017

# Statement

I hereby confirm that I have worked on this diploma thesis on my own just with the methodical support of my supervisor doc. Ing. Marek Foglar, PhD.

In addition I declare that all the references I have used to prepare this thesis are stated in the bibliography.

In Prague, 21st May 2017

.....  
Fiorella Silvana Salcedo Salinas

# Acknowledgement

First, I would like to thank my supervisor doc. Ing. Marek Foglar, PhD for his support, guidance and motivation since the moment I met him. I adress many thanks to the Czech Technical University in Prague for hosting me and for making my my master studies enjoyable.

Also I would like to thank those whom I met during my studies and helped made this time away from home more pleasant.

Last but not least, I would like to thank my mom for her selfless support throughout my studies. Without her love, support and encouragement this achivement would not have been possible.

# Content

<i>1. Introduction</i>	<i>11</i>
4.1. Introduction	11
4.2. Objective of dissertation	12
4.3. Organization of dissertation	12
<i>2. Principles of pre-stressed concrete</i>	<i>13</i>
4.1. Methods of pre-stressing	13
2.1.1. Pre-tensioning Methods	13
2.1.2. Post-tensioning Methods	15
4.2. Materials for pre-stressed concrete	17
2.2.1. Concrete	17
2.2.2. Pre-stressing tendons	19
2.2.2.1. Losses of prestress in the tendons	20
2.2.3. Anchorages and splices	20
2.2.4. Reinforcement steel	22
2.2.5. Sheaths	23
4.3. Durability	23
2.3.1. Corrosion of steel	24
2.3.1.1. Corrosion of the reinforcement steel	24
2.3.1.1.1. Prevention	24
2.3.1.2. Corrosion of pre-stressing steel	25
2.3.1.2.1. Prevention	25
2.3.2. Deteriorating of concrete	26
2.3.3. Grouting	27
4.4. Pre-stressing in buildings	28

2.4.1.	Types of pre-stressed slabs _____	30
3.	<i>Analysis of the structure</i> _____	32
4.1.	Description of the structure _____	34
4.2.	Method of analysis _____	35
4.3.	Modeling of the structure _____	35
3.3.1.	Model 1 _____	35
3.3.1.1.	Input data _____	35
3.3.1.2.	Results _____	36
3.3.2.	Model 2 _____	37
3.3.2.1.	Input data _____	37
3.3.2.2.	Results _____	37
3.3.3.	Model 3 _____	38
3.3.3.1.	Input data _____	38
3.3.3.1.1.	Load patterns _____	39
3.3.3.1.2.	Load combinations _____	41
3.3.3.2.	Results _____	41
3.3.3.2.1.	Results of analysis for dead load + load pattern 1 _____	43
3.3.3.2.2.	Results of analysis for dead load + load pattern 2 _____	44
3.3.3.2.3.	Results of analysis for dead load + load pattern 3 _____	46
4.4.	Results of analysis for dead load + load pattern 4 _____	47
4.5.	Results of analysis for dead load + load pattern 4 _____	49
4.	<i>Reinforcement with pre-stressed concrete</i> _____	55
4.1.	The load balancing method _____	55
4.2.	Detailing _____	57
4.3.	Tendon properties _____	57
4.4.	Loss of pre-stressing due to friction and wobble _____	59

4.5.	Anchorage set loss _____	62
4.6.	Calculation of number of tendons _____	62
4.5.1.	Results for axis F _____	63
4.5.2.	Results for axis H _____	69
4.5.3.	Results for the axis I _____	70
4.5.4.	Results for axis 4 _____	71
4.5.5.	Results for axis 6 _____	71
4.5.6.	Results for axis 7 _____	72
4.6.	Modeling of the pre-stressing _____	72
4.6.1.	Calculation of equivalent loads _____	73
4.6.1.1.	Results for axis F _____	73
4.6.1.2.	Results for axis I _____	75
4.6.1.3.	Results for axis K _____	75
4.6.1.4.	Results for axis 4 _____	76
4.6.1.5.	Results for axis 6 _____	76
4.6.1.6.	Results for axis 7 _____	77
4.7.	Analysis in SCIA _____	77
4.7.1.	Analysis for dead load + load pattern 1 + pre-stress _____	77
4.7.2.	Analysis for dead load + load pattern 2 + pre-stress _____	79
4.7.3.	Analysis for dead load + load pattern 3 + pre-stress _____	81
	_____	83
4.7.4.	Analysis for dead load + load pattern 4 + pre-stress _____	83
4.7.5.	Analysis for dead load + load pattern 5 + pre-stress _____	86
4.8.	Assessment of results and check _____	87
4.8.1.	ULS check _____	88
4.8.2.	SLS check _____	91

<i>5. Conclusions</i> .....	<i>95</i>
<i>References</i> .....	<i>96</i>
<i>ANEX I: Specifications for the Flat GDP plastic duct (DYWIDAG)</i> .....	<i>99</i>

## List of tables

Table 2-1 Dimensions for different types of pre-stressed slab [9] .....	32
Table 3-1 Elevation section of NTK .....	34
Table 3-2 Maximum deflections of 3rd floor slab for the SLS .....	51
Table 3-3 Values for bending moment and torsion .....	53
Table 3-4 Design of conventional reinforcement for slab .....	55
Table 4-1 Calculation of friction loss in axis F .....	65
Table 4-2 Determination of number of tendons for axis F .....	66
Table 4-3 Summary of determination of number of tendons for axis F .....	68
Table 4-4 Summary of determination of number of tendons for axis H .....	69
Table 4-5 Summary of determination of number of tendons for axis I .....	70
Table 4-6 Summary of determination of number of tendons for axis 4 .....	71
Table 4-7 Summary of determination of number of tendons for axis 6 .....	72
Table 4-8 Summary of determination of number of tendons for axis 7 .....	72
Table 4-9 Calculation of equivalent forces for pre-stressing in axis F .....	74
Table 4-10 Calculation of equivalent forces for pre-stressing in axis I .....	75
Table 4-11 Calculation of equivalent forces for pre-stressing in axis K .....	75
Table 4-12 Calculation of equivalent forces for pre-stressing in axis 4 .....	76
Table 4-13 Calculation of equivalent forces for pre-stressing in axis 6 .....	76
Table 4-14 Calculation of equivalent forces for pre-stressing in axis 7 .....	77
Table 4-15 Comparison of deflection with and without pre-stress .....	88

Table 4-16 Conditions for SLS check .....	91
Table 4-17 Moment in y axis on point B.....	88

## List of Figures

Figure 1-1 Principal of pre-stressing .....	11
Figure 2-1 Method of pre-stressing .....	13
Figure 2-2 Hoyer long line system of pre-stressing [4] .....	14
Figure 2-3 Jacking of the tendon .....	16
Figure 2-4 External tendons.....	16
Figure 2-5 Steam curing of hollow-core slabs .....	18
Figure 2-6 Pre-stressing bar .....	19
Figure 2-7 7-wire strand .....	19
Figure 2-8 Methods to attach the bars to the anchor plate [11] .....	21
Figure 2-9 Dead-end anchorage.....	21
Figure 2-10 Types of splices [4] .....	22
Figure 2-11 Corrugated steel ducts .....	23
Figure 2-12 Corrugated plastic ducts.....	23
Figure 2-13 Types of precast pre-stressed slabs.....	28
Figure 2-14 Layout of post-tensed cast-in-place slab .....	29
Figure 2-15 Types of pre-stressed slabs.....	31
Figure 3-1 Facade of NTK.....	33
Figure 3-2 five-story open atrium .....	33
Figure 3-3 Model 1 .....	36



Figure 3-4 Message from model 1 in SCIA.....	36
Figure 3-5 Model 2 .....	37
Figure 3-6 Error in the column capitals in model 2 .....	37
Figure 3-7 Elevation view of 6 m diameter column capital in mm in model 3 .....	38
Figure 3-8 3D view of column capital in model 3 .....	38
Figure 3-9 Model 3 .....	39
Figure 3-10 Load patterns for variable load.....	40
Figure 3-11 My diagram for load pattern 1 before averaging strips.....	41
Figure 3-12 Calculation of averaging strip for 700mm diameter column .....	42
Figure 3-13 Diagrams for dead load + load pattern 1 .....	44
Figure 3-14 Diagrams for dead load + load pattern 2.....	45
Figure 3-15 Diagrams for dead load + load pattern 3 .....	47
Figure 3-16 Diagrams for dead load + load pattern 4.....	49
Figure 3-17 Diagrams for dead load + load pattern 5 .....	51
Figure 4-1 Real force action of tendon on concrete .....	55
Figure 4-2 Equicalent load.....	56
Figure 4-3 Distribution of horizontal and vertical components of pre-stressing force when P=const .....	56
Figure 4-4 Flat Multiplane Anchorage (DYWIDAG) .....	58
Figure 4-5 Plan of analyzed slab.....	58
Figure 4-6 Flat Multiplane Anchorage (DYWIDAG) .....	iError! Marcador no definido.
Figure 4-7 Detail of slab section.....	59
Figure 4-8 Tensile strenght for 7-wire strand .....	59
Figure 4-9 Specifications for 7-wire strands .....	60
Figure 4-10 Three parabola profile.....	60
Figure 4-11 Four parabola profile .....	61
Figure 4-12 Diagram for dead load + load pattern 1 + pre-stress.....	79
Figure 4-13 Diagram for dead load + load pattern 2 + pre-stress .....	81
Figure 4-14 Diagram for dead load + load pattern 3 + pre-stress .....	83
Figure 4-15 Diagram for dead load + load pattern 4 + pre-stress.....	85
Figure 4-16 Diagram for dead load + load pattern 5 + pre-stress .....	87

## Abstract

---

In this thesis, the concrete layout of the National Technical Library (Annex #) was given in order to develop a solution for the structural design of the slab. The architectural layout of slab was visually analyzed to understand its complexity. Next, the model of the structure in the finite element software SCIA Engineer was done to evaluate more in depth the structural behavior of the slab against the imposed loadings. Three models were prepared before obtaining one that could show proper results. For the first model, some interesting features of the software were used to model the structure as similar as possible to the real one but the model was not working, thus, the model was simplified. With this results the possibility of using conventional concrete for the design of this slab was assessed. The main indicator used for this purpose was the long-term deflection of the slab, which resulted more than the permitted limit. As expected, the solution of the structure with conventional reinforced concrete was not possible.

Therefore, it was decided to use pre-stressed concrete to reinforce the structure given the characteristics of the architecture. The method used for the design and modeling was the load balancing method. The pre-stressed reinforcement was designed to balance 80% of the dead load and then modeled in SCIA Engineer. Finally, the results were checked in the Ultimate limit state and the Serviceability limit state.

# 1. Introduction

---

## 2.1. Introduction

The technique of pre-stressing consists in creating an additional stress in a material before being put in service that helps it cope better with the external loads and enhances its performance. In the case of concrete, consists in applying a compressive stress that balances the tensile stress to improve its performance against big tensile stresses, cracking and deflections. (Figure 1-1)

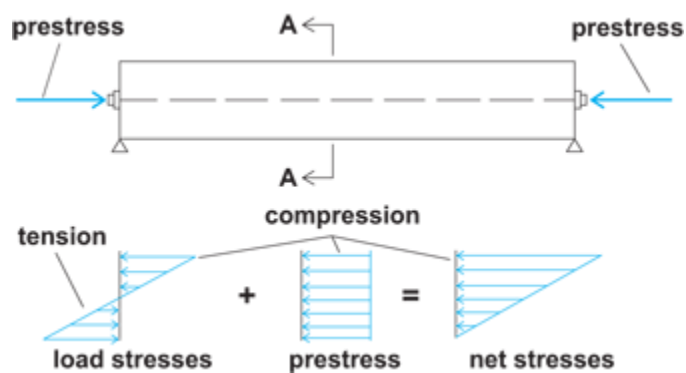


Figure 1-1 Principal of pre-stressing

The forces are transmitted to the concrete through tendons that are usually made of steel. These tendons are pulled with a jack and then anchored to the element. They can be internal tendons embedded or in ducts inside the concrete section or alongside the concrete as external tendons. We can find two types of procedures according to the moment in which the pre-stressing force is applied: pre-tensioning and post-tensioning.

Pre-tensioning consists in stretching the tendons against an anchored formwork before the concrete is poured. Then the tendons are released when the concrete has hardened and reached sufficient strength. The force is transferred to the element by the bond between the concrete and the strands. Pre-tensioning is applied in products like roof slabs, floor slabs, piles, poles, bridge girders, etc. [1]

In the other hand, post-tensioning consists in stretching the tendons after the concrete is already hardened. The internal tendons are placed inside a duct and when the concrete has already reached sufficient strength, the tendons are tensioned with a jack. The force is

transferred to the element by anchoring the tendons at the ends with an anchored plate. If external tendons are used they are installed in ducts placed outside the concrete section. [2] Post-tensioning is used in structural products like large girders, pavements, pressure vessels, floor slabs, and shells, among others. It is very versatile, and usually used in cast in place elements but it can also be used for factory-made products. [1]

Nowadays, it is a very important technique very widely used in structural engineering. This tool has several applications, for example in buildings, concrete bridges, marine structures, floating structures, concrete piles, pressure and containment vessels, etc. In this dissertation the application in buildings will be developed more in depth.

## **2.1. Objective of dissertation**

The aim of this dissertation is to analyze and design the structure of the National Library of Technology (NTK from now on).

First of all, the specific objective are to get familiar with the pre-stressing technology, construction process and durability considerations applied to building construction.

The second specific objective is to demonstrate that the structural design of the typical slab of this building using conventional concrete is not possible in order to prove the limitations of this technology in comparison with pre-stressed concrete.

The third objective is to evaluate the capability of the software SCIA to model and analyze complex structures like the one assessed in this thesis.

Finally, the fourth objective is to present a solution for the structural design of the aforementioned slab using post-tensed concrete.

## **2.2. Organization of dissertation**

This work consists of five chapters. In chapter one the introduction and the aim and objectives of this thesis is presented. Chapter two is an overview of the construction technology, materials used and considerations for the durability of pre-stressed concrete, as well as an introduction to pre-stressing in slabs. In chapter three the structure analyzed

in this thesis is presented and the possibility of reinforcement with conventional concrete is investigated. Chapter four is the design and check of the design of the typical slab using pre-stressed concrete. Finally in chapter five, conclusion and recommendations inferred from this thesis are presented.

## 2. Principles of pre-stressed concrete

---

In this chapter, the methods and construction process of pre-stressing, the most relevant aspects of the materials used in this technique, some consideration about the durability and how pre-stressed concrete is used in building structures will be presented.

### 2.1. Methods of pre-stressing

#### 2.1.1. Pre-tensioning Methods

Pre-tensioning is used primarily in precast elements manufactures in a factory or plant. The tension is applied by hydraulic jacks or by movable stressing machine. High early-strength concrete is used to facilitate early stripping and the reuse of forms. Strands of up to 18mm or tensile wires of up to 7mm anchor themselves by the surface bond and

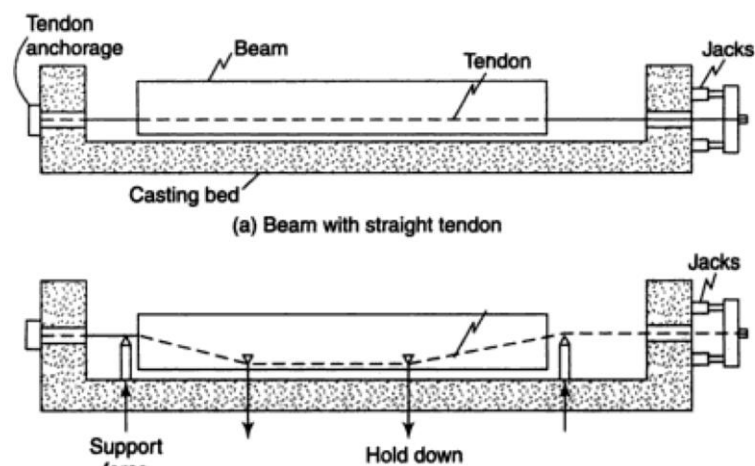


Figure 2-1 Method of pre-stressing

interlocking of the surface indentations. External anchorages are not generally used but when single wires of large diameter are used (more than 7mm), it may be required. The tendons can be stretched with constant or variable eccentricity like in the figure 2.1.

For mass production of pre-stressed elements, Hoyer long line process is used. The tendons are stretched between two anchored blocks several hundred meters apart to allow a large number of elements to be pre-tensed. Figure 2.2 [4]

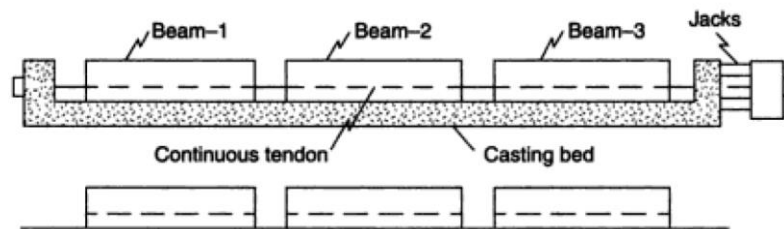


Figure 2-2 Hoyer long line system of pre-stressing [4]

Thermo-electrical pre-tensioning uses electrical heated wires which are anchored before placing the concrete. They are subjected to temperatures of 300-400 °C for 3-5 min. They suffer an elongation and, when cooled, the tendon try to shorten but they are fixed at the ends with an anchorage. With this process it is possible to induce stresses of 500-600N/mm<sup>2</sup>. [4]

Chemical pre-tensioning uses expanding admixtures in the concrete and it induces a linear expansion of 3-4 %. The expansion is restrained by the high-tensile steel wires which generates tensile forces in the wire. Chemical pre-stressing is ideal for columns, pipes, thin walls, slabs or shells. This method is not intended for high pre-stress application. [4]

One advantage of pre-tensioning precast concrete is that factory production ensures good quality of the product and minimize geometrical defects on the elements. It also allows the casting of the precast products and other stages of the project, like the foundations, to progress simultaneously. Also falsework is not necessary since the members are not cast on the site, reducing costs and facilitating the construction.

### 2.1.2. Post-tensioning Methods

Post-tensioning is ideal for medium to long-span in situ works where the tensioning cost is only a small proportion of the total cost. Thus, is more economical to use a few cables or bars with large forces in each than more small members.

First, horizontal cast-in-place members are supported by shoring. Shoring must be strong enough to support all dead loads and lateral loads due to construction operations. Forms also have to be designed in order to resist the pressure of the fresh concrete, which are high due to the use of water reducing admixtures. They also have to allow the change of volume due to shrinkage and the deformations due to the pre-stressing.

Second, the mild steel reinforcement is placed. Then, metal ducts or corrugated high density polyethylene (HDPE) ducts and anchorages are installed. This technique requires accurate location of the pre-stressing force so this must be done carefully. The tendons can be placed through the ducts after pouring the concrete or can be pre-placed when fixing the ducts. [9]

Afterwards, concrete is placed and thoroughly compacted. Concrete is cured to accelerate strength gain. When concrete has hardened, the stressing of the tendons takes place (fig 2.3). In most cases stressing is done from 2 to 7 days after casting. [9] Finally the duct is filled with a colloidal grout to establish the bond and protect the tendon in a process called “grouting”, which will be further explained in 2.3.3. If the possibility of posterior change of tendons in case of deterioration or additional stressing in the future is desired, this is possible with the use of external tendons (fig 2.4). The cables are external and the

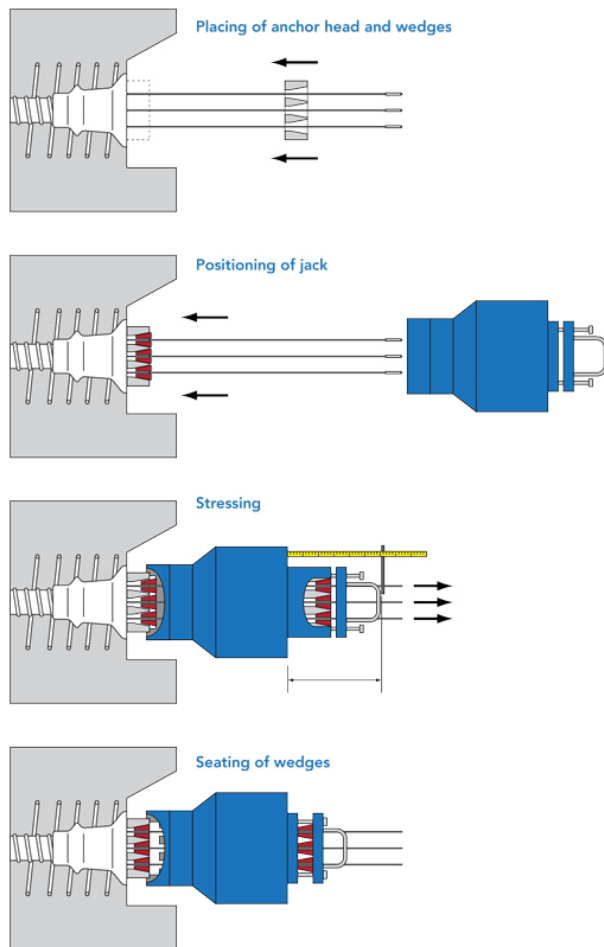


Figure 2-3 Jacking of the tendon



Figure 2-4 External tendons

eccentricity is varied using saddles at appropriate places to obtain the required profile. There is no bond between tendons and concrete. It avoids congestion of reinforcement and it allows the section area to be smaller since is not necessary to include space for the duct.



It can be used for applying pre-stress in existing structures as improving its performance. [9]

## 2.2. Materials for pre-stressed concrete

The main materials used in pre-stressed concrete are the concrete, pre-stressing tendons, reinforcing steel and the anchorage.

### 2.2.1. Concrete

For the purpose of pre-stressing concrete, the concrete should develop high strength in an early age, low creep characteristics through time, low shrinkage and a high elasticity modulus. [4] Also the creep, the shrinkage and the pre-stressing losses depend of the strength of the concrete. This can be achieved having special attention to the aggregates, admixtures, the placing and the curing.

A high strength concrete must have the lowest water content and should be suitable for compaction by the means of the site. [4] With the especially dry mixes employed in pre-stressed concrete, intensive vibration is necessary to fill the voids especially in congested areas. [1] Internal vibration is the most used technic but external or form vibration is also effective in thin products. This processes can produce a deflection or change of position in the reinforcement if not carefully controlled.

The shrinkage of the concrete is caused by the gradual loss of moisture that results in a change of volume. It depends on the aggregate type, relative humidity, W/C ratio and ratio of surface area to volume. Mixes with high cement content are prone to exhibit bigger shrinkage because of the contraction of the cement gel. The value of the shrinkage will be bigger in pre-tensioned steel than with post-tensioned steel because in the first one we have to take into account the total shrinkage whereas in the second one we will just take into account the shrinkage from the moment the load was applied. The use of low weight aggregates will also increase the shrinkage value. [4]

Curing is very important in developing an initial high strength and it also allows the completion of the chemical reactions that produce strong durable concrete. It also

prevents the loss of moisture that causes the initial shrinkage. Some of the techniques used are fog spray, covering with an impervious blanket, covering with a wet burlap, low-temperature low-pressure steam or spraying a membrane curing compound. [1] In the figure 2.5 we can see hollow core slabs being cured with steam.

Admixtures, specifically water reducing, are very effective in reducing the W/C ratio. This is important in order to produce a high strength concrete with adequate impermeability,



*Figure 2-5 Steam curing of hollow-core slabs*

low shrinkage and hence good durability. It also improves the workability which makes it easier to compact. Other type of admixtures used in pre-stressed concrete are accelerating admixtures to reduce the time before the pre-stressing can be held, to inhibit corrosion of the reinforcement, and air entrainment admixtures to improve the performance against freeze-thaw attack.

Selection of the aggregate is also fundamental. Crushed rock improves the aggregate-paste bond better than gravel. The maximum size should be kept small as of 20mm or 10mm for very high strengths. Aggregate should be clean from silt and dust that can damage the concrete.

### 2.2.2. Pre-stressing tendons

The tendon is the mean to produce the compressive strength and it should have high tensile stress and sustain indefinitely a high state of stress. The materials used for this purpose are usually cold drawn steel or alloy steel.

Several types of pre-stressing steel can be found.

- Bars having a diameter of 15 to 50 mm (fig 2.6). The steel ranges from Y1030H to Y1230H, where the number represents the tensile strength in N/mm<sup>2</sup>. The bars are made from hot rolled steel (code H). They can be plain (code P) or ribbed (code R), the latter having better bond. One advantage of bars is that they can be cut and anchored at any position or can be extended by coupling. [11]



Figure 2-6 Pre-stressing bar

- Wires with a diameter of 3 to 10 mm. They are cold drawn (code C) and the steel ranges from Y1570C to Y1860C. [11]
- Strands made from three to seven wrapped wires. It consists in an individual wire with other six wires twisted around inner core wire. The diameter of the wires are between 2 to 5 mm and the central bar has around 2% more diameter than the other six. Steel



Figure 2-7 7-wire strand

ranges from Y1670 to Y2160. The number of wires in the strand is represented in the code, e.g. Y1670S7 having 7 wires. [11] 7-wire strands are the most common form of tendon. (Figure 2-7). This wires comes with and indent to increase bond. A typical posttensioning assemblage consists of 19 or 37 strands of 15mm diameter. The tendons can be galvanized or epoxy coated if greater protection required.

### 3.2.2.1. Losses of prestress in the tendons

However, tendons present a loss of stress which takes place in two stages. First, pre-stress applied at the time of jacking is reduced immediately after jacking due to elastic contraction of the tendon. In post-tensioned concrete there is loss due to friction between the ducts and the cable from the jacking end to the anchored end. There is also some loss due to slip at the anchors. Then, over a period of time, creep, shrinkage and relaxation of steel create an additional loss of stress. Finally the losses are of the order of 25% of the initial jacking force. This losses must be taken into account in the design. [9]

### 2.2.3. Anchorages and splices

In pre-tensioned concrete the anchorage is by bond of the tendon in the concrete but for posttensioned tendons the anchorage is achieved by gripping or securing the tendons in the ends of the structural element. There is plenty of devices to be used in pre-stressing anchoring since mostly all anchorages are part of proprietary systems for post tensioning. [1] The most widely used are:

- Anchorage by means of anchor plates. The bars can be attached to the anchor plate with split-wedge anchorages, with upsetted heads or with nuts, as shown in figure 2.8.
- Strand dead-end anchorage in which the strands are spread out in the end (fig 2.9).
- Anchorages with swaged fitting with epoxy or cement mortar

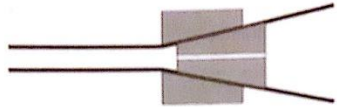
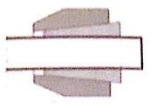
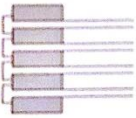
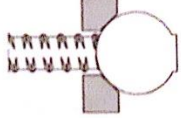
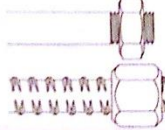
Type	Wire	Strand	Bar
Anchoring			
Wedges			
Upsetted heads			
Nut			

Figure 2-8 Methods to attach the bars to the anchor plate [11]

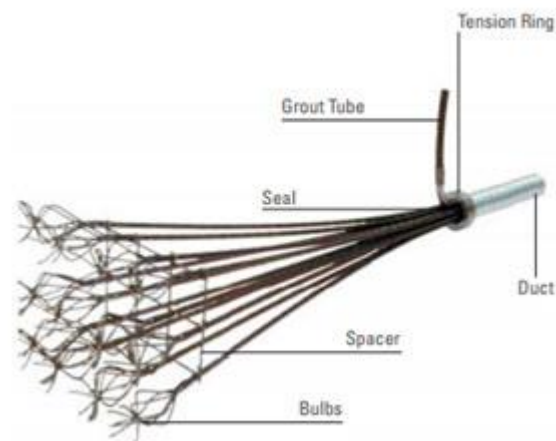


Figure 2-9 Dead-end anchorage

Also tendons can be coupled with splices to extend their length when needed. It also needs to ensure full transfer of forces between the bars. Some of the most commonly used can be found in figure #. The most used is the screw connector: a coupler with female threads that screws in the end of both bars.

Due to the dimensions of the forces used in pre-stressing, it is extremely important that the anchorage and splices works safely. Anchorages should be protected from fire or corrosion. It is essential that anchorages are aligned axially to the tendons. Manufacturer recommendations must be thoroughly followed. In the use

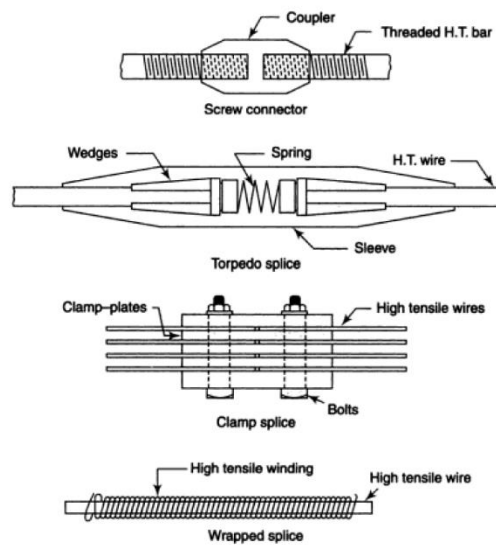


Figure 2-10 Types of splices [4]

#### 2.2.4. Reinforcement steel

Reinforcement steel is classified as the “passive steel”. It confines the pre-compressed zone, resists secondary tensile stresses and provides resistance to transverse and torsional shear. It comes in sizes up to 35 or sometimes up to 50 mm and, according to the yield strength, ranges from 300 to 500 MPa.[1]

Due to the heavy vibration required in pre-stressed members, is very usual that steel bars are dislocated either by concrete placement or by the vibration. This can be prevented by proper tying and “dobe” blocks. The latter, together with plastic chairs, is also used to maintain the specified cover in order to prevent corrosion. [1]

Pre-stressed members will behave as designed only if carefully detailed and placed so installation, positioning and securing of reinforcing bars becomes essential. [1]

### 2.2.5. Sheaths

Sheaths are used in internal posttensioning and they create a void inside the cross section in which the tendon is going to be placed. They can be made from corrugated steel (Figure 2-11) or from corrugated plastic ducts (Figure 2-12), the latter being more durable since they are water tight along the whole length, they are flexible enough for normal curvatures and they are inert in the concrete. They can also be easily spliced or joined in the field. The performance of plastic tendons are satisfactory for this purpose. Ducts are also used in external posttensioning as high-density polyethylene ducts (HDPE).

Grout inlets, outlets, vents and drainage tubes are needed along the ducts for drainage of any water and for grouting.



Figure 2-11 Corrugated steel ducts



Figure 2-12 Corrugated plastic ducts

### 2.3. Durability

To provide a long design life to the pre-stressed concrete, attention must be given to concrete and the tendons through well design details and construction practices in order to protect them from the environmental attacks. As a matter of fact, pre-stressed buildings and elements present good durability because it prevents cracking which is one of the most usual ways in which durability is jeopardize. The most common environmental

attacks, in the case of the concrete, are the sulfate attack, freeze-thaw attack, thermal cracking and shrinkage. In the case of the steel is mainly the corrosion. How this factors affects the elements and the measures that need to be taken to prevent its deterioration will be presented.

### **2.3.1. Corrosion of steel**

#### **3.3.1.1. Corrosion of the reinforcement steel**

Initially when the steel is surrounded by concrete, a thin coat of ferro-ferrous hydroxide is formed around the surface of the steel which passivates the surface. It remains passivated until an external action like carbon dioxide from the air penetrates and the passivating layer dissolves.

However, chlorides are the most aggressive elements to steel. Chlorides can be found in seawater or salt air. Chloride ions penetrate by capillary action and diffusion through the concrete and when it reaches the steel, it dissolves the passivating layer. [1] Once this layer is destroyed and oxygen molecules also reach the steel the process of corrosion initiates and it remains in the life of the structure depending on how fast the corrosion develops.

For structures below water or soil level, availability of oxygen is limited so corrosion will not develop rapidly. The structures that are exposed to intermittent states of wet and dry are more prone to present corrosion, joined to the fact that it produces micro-cracking in the structure and increases permeation of chloride ions and oxygen. Therefore, the penetration of chlorides depends of the permeability of concrete. [1]

##### **3.3.1.1.1. Prevention**

As previously stated, in order to protect the steel from corrosion is essential to produce impermeable concrete. This can be achieved with the following measures:

- Reduction of the W/CM rate, which reduces permeability and increases resistivity.
- Use of nonpermeable aggregates of small maximum size.
- Use of a Portland cement containing 6 to 10% of C3A, because it combines with the chloride ions and forms insoluble cloro-aluminates particles which block the pores. [1]



- Proper curing, since it reduces cracking and promotes full hydration of cement paste which improves the surface skin.
- Minimizing thermal strains because of the heat of hydration by, for example, precooling the aggregates or using cement that generates less heat.
- Impregnation of surface or the use of coatings in the surface

Coupled with a permeable concrete, the treatment of construction joints are also a way for chlorides, water or oxygen to reach the steel. Preparing a proper surface between the joints by high pressure water jetting, wet sandblasting or wire brushing after initial set is a good idea.

Epoxy or other types of coating is also available to protect the reinforcement bars. Bending of the bars can crack the coating but it does not lead to corrosion since the area is usually very small. This coatings do not allow the bars to have bond to transfer stresses, they rely only on deformation to transfer stress. Nevertheless, fine sand embedded coatings can be used to improve bond.

Provision of adequate cover, the use of small reinforcing bars instead of one large bar and reducing the entrapped air in order to minimize internal voids are other measures to be taken to prevent corrosion.

### **3.3.1.2. Corrosion of pre-stressing steel**

Any loss of area of the cross section of the tendon caused by corrosion is critical since the value of the stress used are very large. Pre-stressing steel wires, bars and strands are usually uncoated, however is very important to protect them during the transportation, storage, loading and structural life. In pre-stressed tendons, additionally to corrosion from chlorides and carbonation, presents two types of corrosion: stress corrosion and hydrogen embrittlement. But this two has been almost eradicated by good construction practices and quality assurance.

#### **3.3.1.2.1. Prevention**

The tendons are vital materials made out of bright steel which is susceptible to atmospheric corrosion if exposed enough, hence is important not to take it out from storage more than 24 hours before the placing. They can also be coated with soluble oil, which is washed away at

the moment of the grouting. This also reduces loss of friction during stressing. In the case of pre-stressing, the tendons are fully embedded in the concrete so they are well protected against corrosion. The ends can be painted on the ends when they are extended to the concrete surface to ensure water tightness. Anyways, corrosion on the tips of the wire does not extend inwards more than 2 to 3mm. [1]

Metal ducts can also suffer from corrosion which can generate holes that expose the tendons and can block the duct. It also needs to be in protected storage until 1 or 2 days before placing. [1] Special attention must be taken to the splices of the ducts in order to ensure the water tightness.

The pre-stressing materials must be protected throughout the transit, shipping, storage and installation by wrapping and sealing them in watertight packaging, dehumidifying the storage shed by heat or other means and sealing the end of the ducts until grouting. [1]

### 2.3.2. Deterioring of concrete

Alkali-Aggregate reaction is caused by the chemical reaction between reactive silica and the alkali found in the cement or other external sources. Its consequences are not visible until after many years so it is important to prevent it. Some forms of prevention are by testing the aggregates to see if they have a high percentage of reactive silica or to limit the alkali available in the cement to 0.65%

In concrete exposed to very cold climates, freeze-thaw attack occurs inside the filled water pores when the water freezes creating expansive forces. For typical concrete, after 200 or 300 cycles of freezing and thawing, internal fatigue and spalling of the concrete occur. This can be passivated by the employment of air entraining admixtures. The amount and type of air might be influenced by other admixtures, especially water reducers. [1]

Thermal cracking can also create cracks in the concrete due to thermal expansion of the concrete cause by the heat of hydration of cement. It can also develop in service when there is a differential of temperature between two sides of the element. This is especially severe in elements with thickness from 600mm or more but can also affect thin elements. If there is not

enough reinforcement to pull the cracks closed then it is a path for moisture to reach the reinforcement. Also insulation of the surfaces can be used.[1]

Drying shrinkage is an effect of the evaporation of water in the mix but due to the fact that pre-stressing mixes use a low W/C is unlikely that would happen. Nevertheless, early exposure of unprotected surfaces to drying winds or hot climates must be avoided. [1]

### **2.3.3. Grouting**

Grouting is a practice used for post-tensioned tendons and consists in filling the duct with cement grout throughout its length. It is a very important part of the process of post-tension. It improves the overall durability of the structure, provides bond between tendon and structural concrete, protects the tendon, completes the cross section and impedes water or other external agents to reach the tendon.

Grouting is usually a mix of water, cement and admixtures. The mix should not exceed 0.45 W/C ratio and the duct size should be at least the double of the tendon. For example, in the UK nowadays they use pre-bagged materials with only water measured and added on site. [2]

Bleeding is a problem that occurs in grouting because of the difference of specific gravity between the water and the cement. This causes sedimentation of the cement and water emerges from the grout. Bleeding water gets trapped in the duct and, when freeze, can create pressure on the ducts and produces air voids. Material, mixtures, admixtures and injection procedures must be chosen to minimize bleeding.

Expansion of the grout is used to ensure filling all the voids in the ducts. This can be achieved with expanding admixtures. The expansion should not exceed 10% to prevent an excess of expansion force inside the duct.

The best assurance of the grout properties is through different tests held after mixing and before installation. The properties like bleeding, fluidity, sedimentation, volume changes and strength are tested [2]. The ducts are also tested before grouting to ensure there is no leakage. Air pressure and water pressure testing are used for this purpose.

First water is drained out of the duct, then grout is slowly inserted through the inlet left in the anchorage with a pressure of 0-1N/mm<sup>2</sup>. Grout emerges from intermediate vents along the element before they are sealed. A quantity of grout is allowed to vent from the intermediate vents and the outlet at the end, approximately 100% of the volume of the duct is wasted [1]. The air retained in the duct comes out from the vents as bubbles and outlets are closed when no more bubbles are visible. Then the wasted grout is collected and subjected to fluidity tests. [2]

In the case of unbonded tendons, wax and grease grouts are used to ensure future easy destressing, additional stressing or replacing of the tendons. The grout is injected at between 80 and 90<sup>0</sup>C and when it cools it becomes a flexible filler. [2]

## 2.4.Pre-stressing in buildings

The largest use of pre-stressing in buildings is with precast pre-tensioned members, specifically hollow core slabs (figure #) and double tee slabs (figure #). To support the slab, members like the inverted “T” and “L” girders have been developed. Solid flat slabs are also used. The aforementioned types of slab are illustrated in figure 2.13.

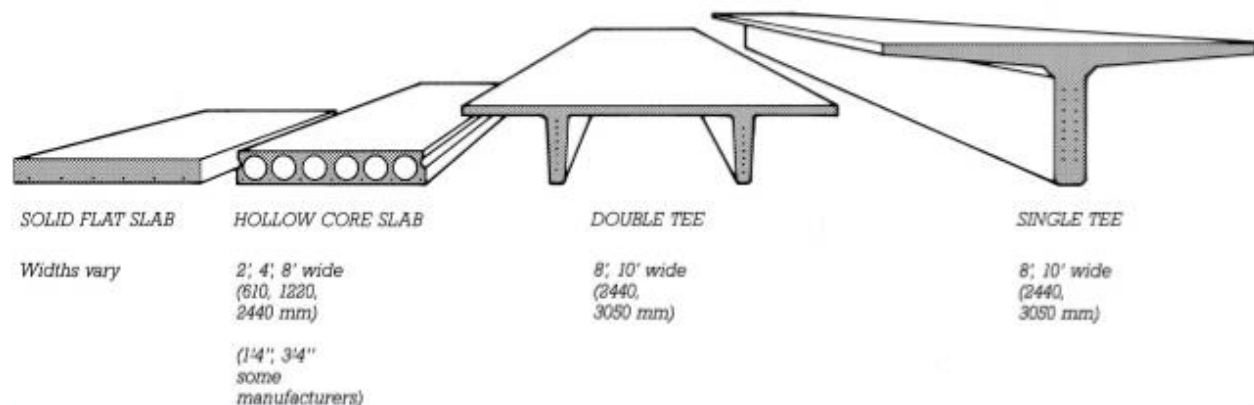


Figure 2-13 Types of precast pre-stressed slabs

Pre-stressed pre-cast hollow-core slabs do not have any shear force reinforcement, hence the shear forces must be beared by the reinforcement web. The mix and the processes must be made to maximize tensile strength of the concrete. This slabs are usually erected by boom

crane or tower cranes and set on walls or beams. A good practice is to include in the wall-to-slab joint reinforcing ties to prevent dislodgement in case of accident.

Double tee slabs are highly structural efficient. For shear reinforcement, it often requires web reinforcement. Welded mesh is usually enough and it improves the anchorage in the ends.

Erection create temporary stresses depending of the method. End support of the members when lifted is not as favorable as the final support, so provision of shear reinforcement in the end zones is a good practice. Pre-stressing elements for building are especially thin so special care in handling must be taken. Control of camber and warping is very important in slender elements.

Connections between precast elements must be designed and execute to perform the function contemplated in the design, permit volume changes due to shrinkage, creep and temperature changes, and accept overloads with ductility throughout the life of the structure. They must ensure adequate corrosion and fire protection.

When it comes to post-tensioned concrete, the most extensive applications are in waffle floor and flat slabs. It not only provides strength but also controls the deflection in service, achieving a truly flat slab. For this purpose, the “load balancing” method is used in which loads are balanced and the upward force of the tendons counteracts the dead and live loads. Hence,

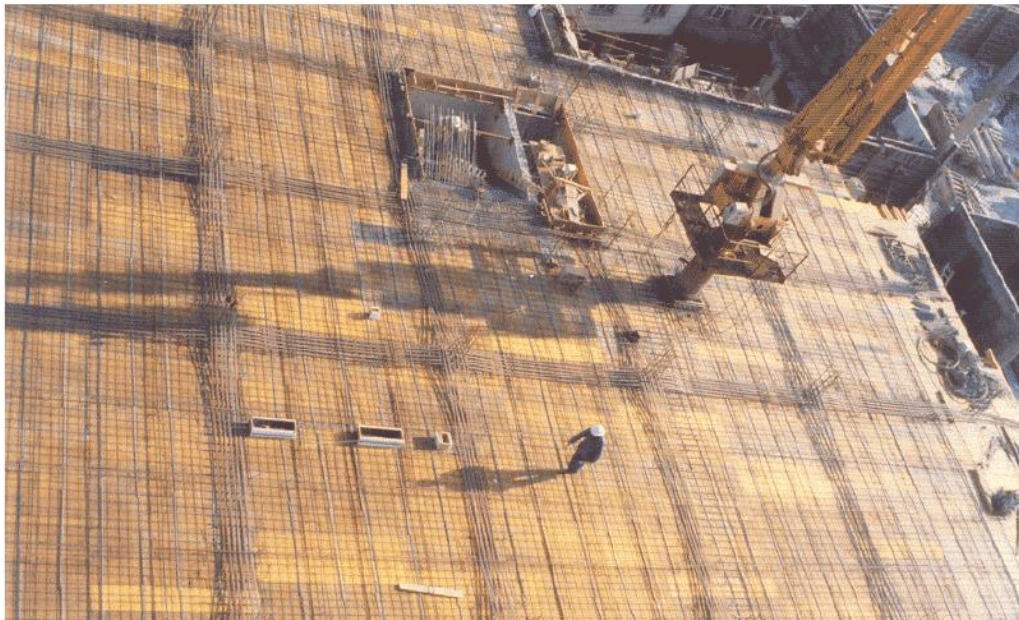


*Figure 2-14 Layout of post-tensed cast-in-place slab*

long term creep does not increase the camber or the sag. [1] This method will be further discussed in chapter 4.

Post-tensioned slabs are cast in place and the tendons are placed in an orthogonal pattern, concentrated in the column lines, as shown in figure 2.13. The tendons are typically unbonded and a single strand is often used. Polyethylene sheaths are used to provide durability. [1]

In building construction, some of the biggest advantages of post-tensioned slabs compared with reinforced concrete is that it makes it possible to achieve longer spans with thinner depth of slab, leading to flexibility of partitions and reduced height of the building. Post-tensioning is also used in foundation slabs, beams and girders.

#### 2.4.1. Types of pre-stressed slabs

Structurally, we can classify them in one-way and two-way slabs. One way slabs are ideal when the span on one direction is bigger than in the other direction. In general, if the ratio longer span/shorter span is less than 2 then we can assume two way slab. Two way slab is ideal where higher live loads are supported and uninterrupted floor space is desirable.

The criteria for two-way slabs is the constraint imposed on upward deflections under pre-stress and self-weight. So that tensile cracks are completely eliminated under service loads. Shear reinforcement are generally not required. Most of the two-way slabs fall in one of the following three categories:

- Edge-supported slabs which have beams or walls along their four edges, with or without restraint.
- Flat slabs are supported on columns without beams in between and reinforced with drop panel or column capital around the columns. They can be flat slabs or waffle slabs.
- Flat plates are solid slabs with constant thickness everywhere. [12]

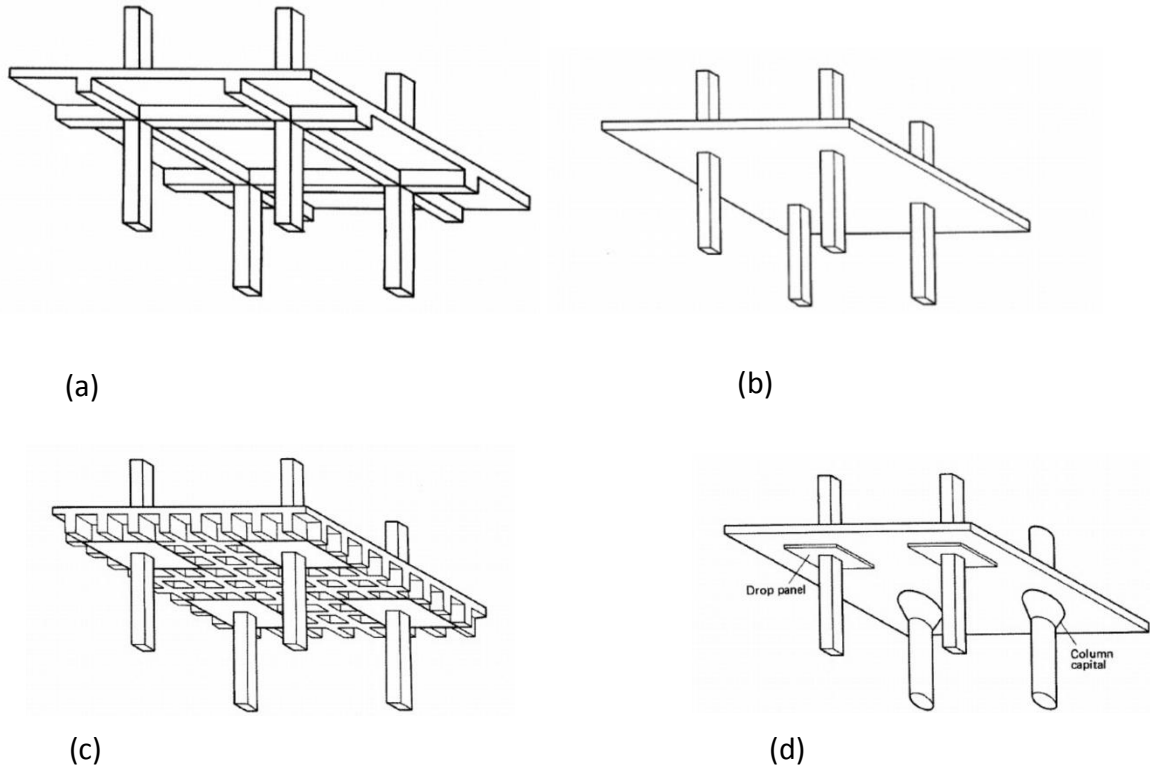


Figure 2-15 Types of pre-stressed slabs

Slab type	Slab span (m)	Slab depth (mm)	Beam depth (mm)	Span/depth ratio, slab/beam
Solid flat slab	6	200		30
	8	250		32
Solid flat slab with drop panels	8	225		36
	12	300		40
One-way slab with band beams	6	150	300	40,20
	8	200	375	40,21
	12	300	550	40,22
One-way slab with narrow beams	6	175	375	34,16
	8	225	500	36,16
	12	325	750	37,16

Ribbed slab	6	300		27
	8	450		27
	12	575		26

Table 2-1 Dimensions for different types of pre-stressed slab [9]

In table 2.1 we can find some dimensions for two-way slabs with an imposed load of 5kN/m<sup>2</sup>.

Flat slabs have the advantage that the formwork is very simple and leads to an uncluttered and more appealing flat soffit. The additional reinforcement around the corners increases the shear capacity. Nevertheless, it can be replaced by a steel shear head within the depth of the slab. This solution is suitable for spans in the range of 6 to 13m. Moreover, post-tensioned waffle slabs can be used to reduce the dead weight of the slab. The slab is solid around the columns to increase the shear capacity. They are used in buildings subjected to heavy loading. Spans in the order of 10 to 20m can be achieved with waffle slabs. [9]

### 3. Analysis of the structure

---

The structure that will be design is the National Technical Library in Prague (fig 3.1). This building is located at Technická 6, Prague 6, Czech Republic. Construction of the current building began in 2006 and was completed in January 2009. The library opened to the public on 9 September 2009 and now boasts the most extensive collection of Czech and international documents in the field of technology and applied natural and social sciences related to technology in the Czech Republic. [5] It was designed by the Projektil Architekti studio and





Figure 3-2 five-story open atrium

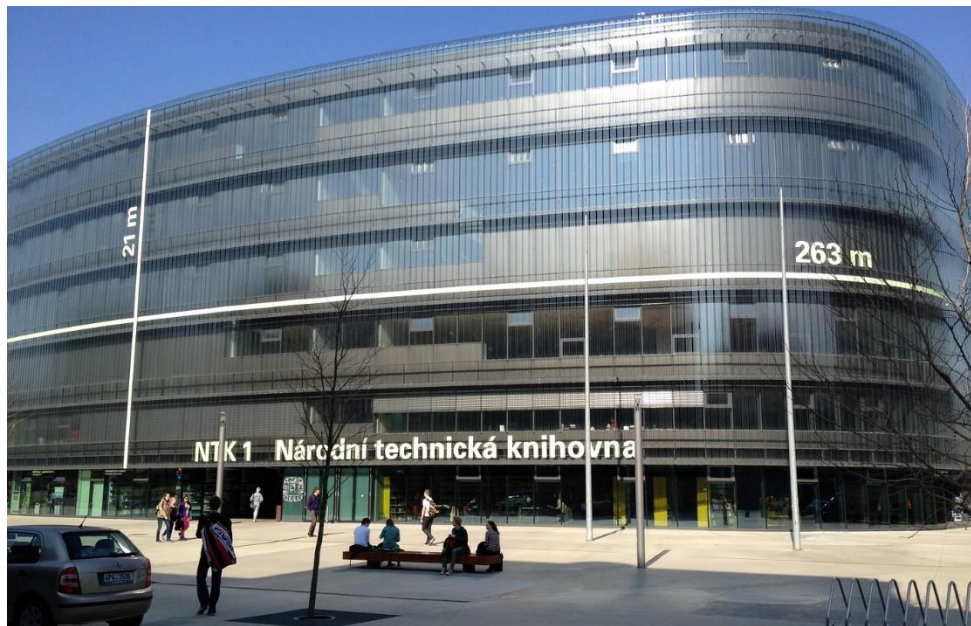


Figure 3-1 Facade of NTK

the building contractor was the partnership Metrostav - OHLŽS. It has 6 aboveground floors and 3 underground floors (fig 3.2). It also has a rectangular, five-story open atrium with stairwells and elevators enabling access to all public areas (fig 3.3). [6]

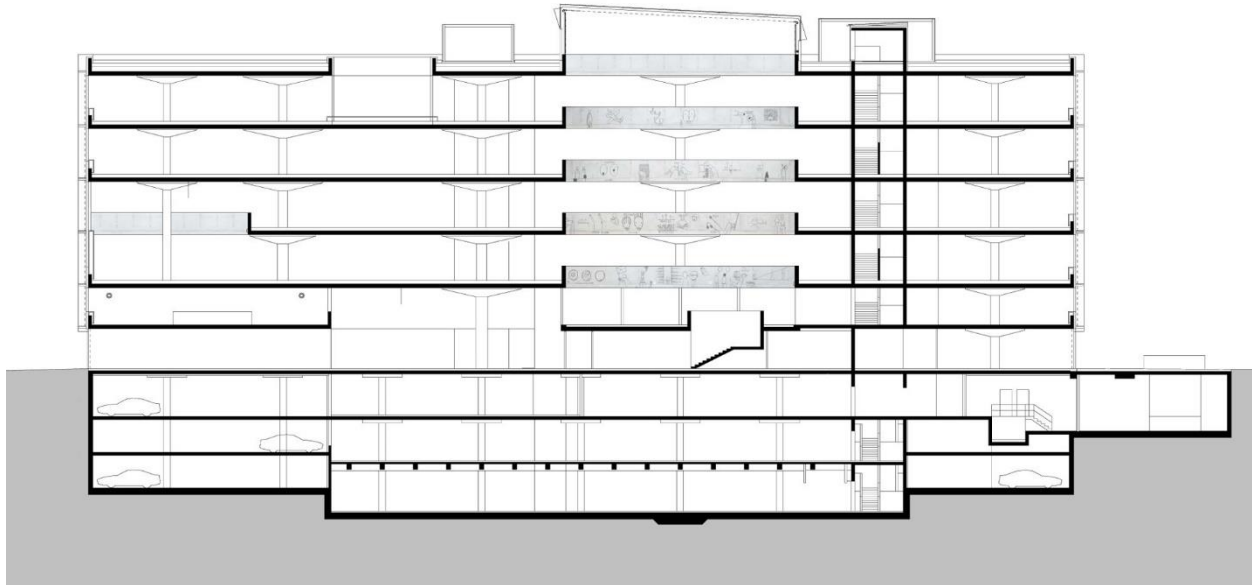


Table 3-1 Elevation section of NTK

## 2.1. Description of the structure

This structure is very complex and unusual. The plan of the second story can be found in the Annex 2

The shape of the structure is curved in all the outside perimeter.

From 3<sup>rd</sup> to 6<sup>th</sup> floor there is an open atrium. The perimeter of the atrium has a concrete parapet in which there is some artwork done.

Tall heights between floors in some places of the library (lobby and 3<sup>rd</sup> floor study area) so must not be heavy because risk of buckling.

15m spans in direction X and Y

Large amount of openings

It has one lift core and four emergency stairs cores.

There is continuity of the columns along the height of the structure.

## **2.2.Method of analysis**

The analysis was focused on the 3rd floor, been the most typical floor of all. It does not have openings. The first four floors will be modeled and an initial assessment of results will be run. The possibility of design using conventional reinforced concrete will be analyzed. If this possibility is not convenient, then

## **2.3. Modeling of the structure**

The structure was modeled in the software SCIA version 16.1.3033. Three models were made before we could retrieve proper results and values.

### **2.3.1. Model 1**

This first model was made using all the features of the software to resemble the original structure as much as possible. The following parameters were inserted in the program.

#### **4.3.1.1. Input data**

The concrete used for the analysis was C40/50. The life load used for a building category E1 was  $7.5 \text{ KN/m}^2$  according to the Eurocode [16]. The life load was applied in the whole slab. As superimposed load, a load of  $1.5 \text{ kN/m}^2$  was assumed taking into account the electric installations and piping. By simple inspection, the building does not have many partitions to be considered. The slab was a 300mm plate. The Autocad plan was inserted in the program and the perimeter of the slab was created with circular arcs following the plan, therefore there was only one slab per floor. The circular column capitals where modeled with the feature “subregion” with variable thickness. The atrium, the stairs shaft and the elevator shaft were modeled as “openings”. Just the first 4 floors where modeled.

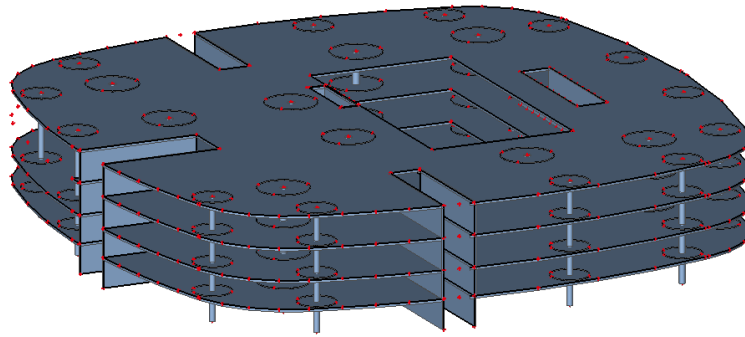


Figure 3-3 Model 1

### 4.3.1.2. Results

I decided to run first a calculation without any combination just to see the nature of the results. When the calculation was run the message in figure # appeared that states that the model was not correct and that it would show the errors via flags in the structure, but no flags were shown. The model was redone and this time the slab was delimited by several straight lines instead of circular arcs, but the message was still appearing.

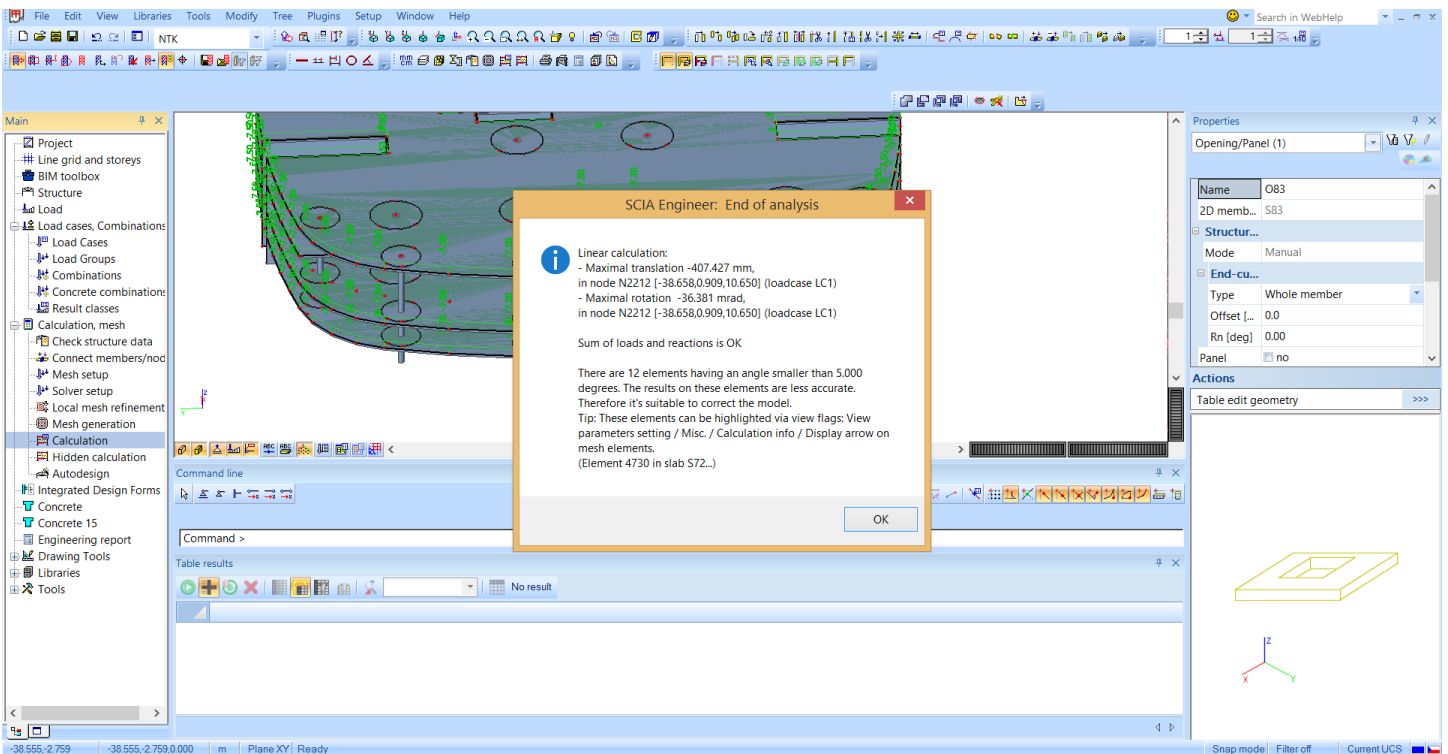


Figure 3-4 Message from model 1 in SCIA

### 2.3.2. Model 2

For this model, the aim was to simplify the structure in order to create less errors.

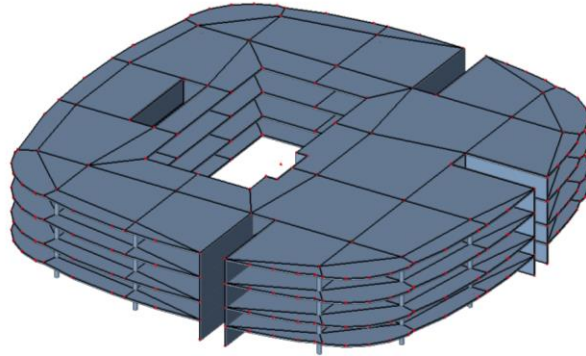


Figure 3-5 Model 2

#### 4.3.2.1. Input data

The loading was the same from Model 1. The slab was delimited with consecutive lines along the perimeter and made from smaller slabs with depth 300mm. The slabs were made respecting the shape of the openings. The column capitals where made with small slabs with depth 100mm and then subregions with variable thickness were created on those slabs.

#### 4.3.2.2. Results

When the structural check was run, the software was separating the column capitals from the slabs. (Figure 3-6) It is very clear that a proper analysis cannot be made if the capitals were not attached to the slab.

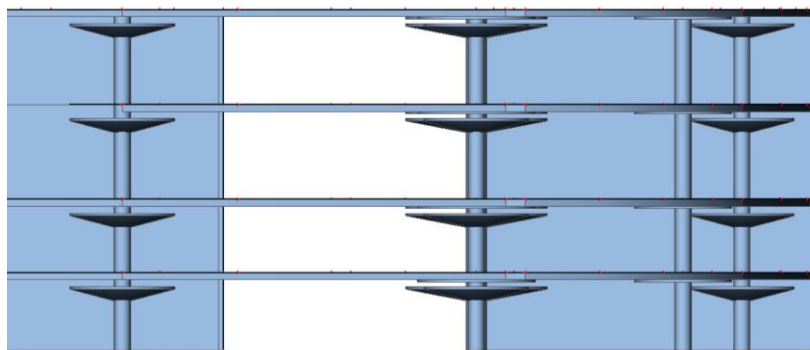


Figure 3-6 Error in the column capitals in model 2

### 2.3.3. Model 3

This time, the model was created as simple as possible. The model was made based exclusively of small slabs forming every floor. No other features were used. (Figure 3-9)

#### 4.3.3.1. Input data

The loading was the same as for the previous models: a superimposed load of  $1.5 \text{ kN/m}^2$  and a live load of  $7.5 \text{ kN/m}^2$ . The slab was made of small slabs of depth 300mm, smaller than the slabs in Model 2, approximately they were  $7.5 \times 7.5 \text{ m}$ . The perimeter of the slab was made with straight lines. The perimeter of the column capitols were made as decagons (Figure 3-8) and the hinge was replaced by a stepped profile with 3 constant thickness (Figure 3-7). The thicknesses were calculated dividing into three the total thickness of the capital and then, with equivalent triangles, the diameter of every concentric slab around the column was determined. The slabs were made leaving space for the shape of the openings.

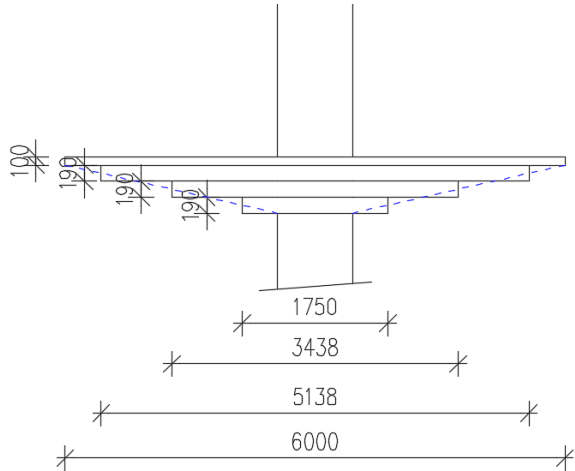


Figure 3-7 Elevation view of 6 m diameter column capital in mm in model 3

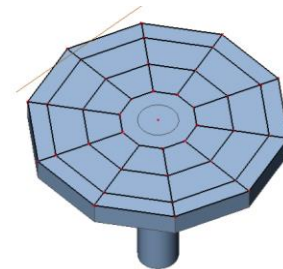


Figure 3-8 3D view of column capital in model 3

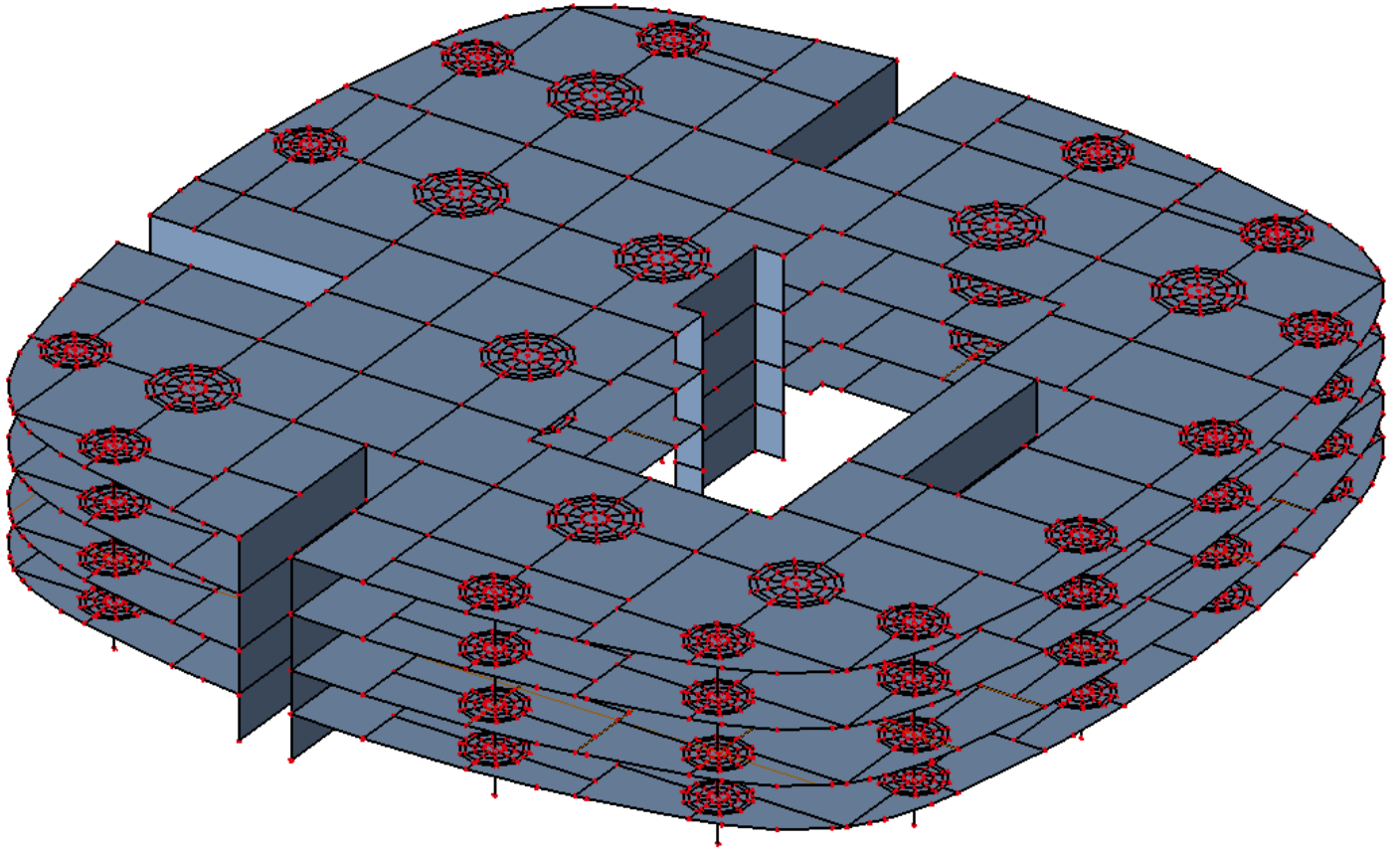
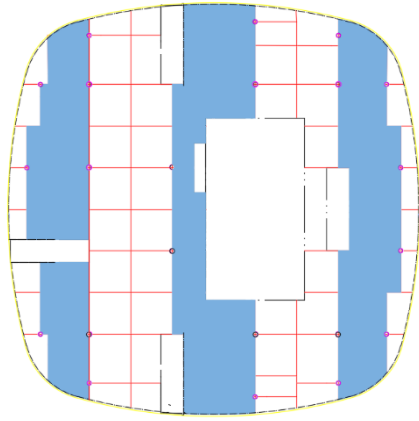


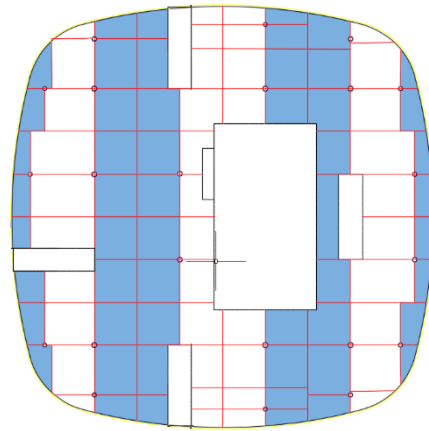
Figure 3-9 Model 3

#### 4.3.3.1.1. Load patterns

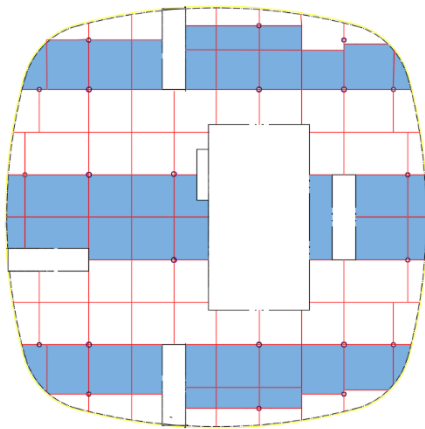
Full factored dead load together with the load patterns shown in Figure 3-10 a-e were considered for the analysis.



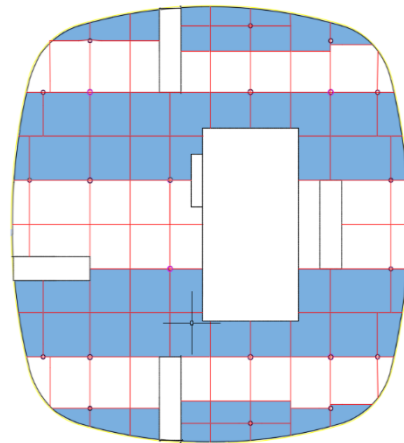
(a) Load pattern 1



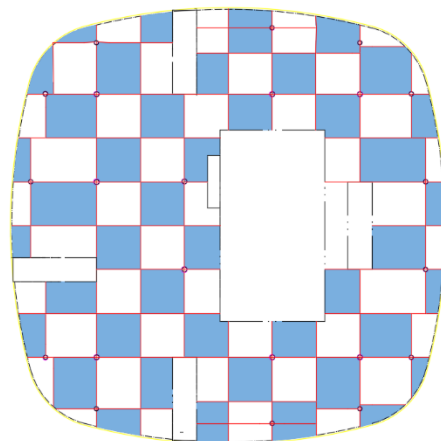
(b) Load pattern 2



(c) Load pattern 3



(d) Load pattern 4



(e) Load pattern 5

Figure 3-10 Load patterns for variable load



### 4.3.3.1.2. Load combinations

For the calculation of effects of load action for the Service Limit State, the combinations  $G_k+Q_k$  for characteristic and  $G_k+\Psi_2Q_k$  for quasi permanent will be used, in which  $\Psi_2=0.8$  for building category E: Storage areas according to the Eurocode.

For the calculation of effects of load action for the Ultimate Limit State, the following combination according to the Eurocode will be used:  $\gamma_G G_k + \gamma_Q \Psi_2 Q_k$ , in which  $\gamma_G=1.35$  and  $\gamma_Q=1.5$ .

### 4.3.3.2. Results

When the structural check was done, no error was shown. The calculation did not show any error either. Nonetheless, some of the negative moments around the columns were giving very high values like in the example for the  $M_y$  (load pattern 1) shown below in Figure 3-11. This occurs because the solutions calculated on this program are based on an elastic analysis but

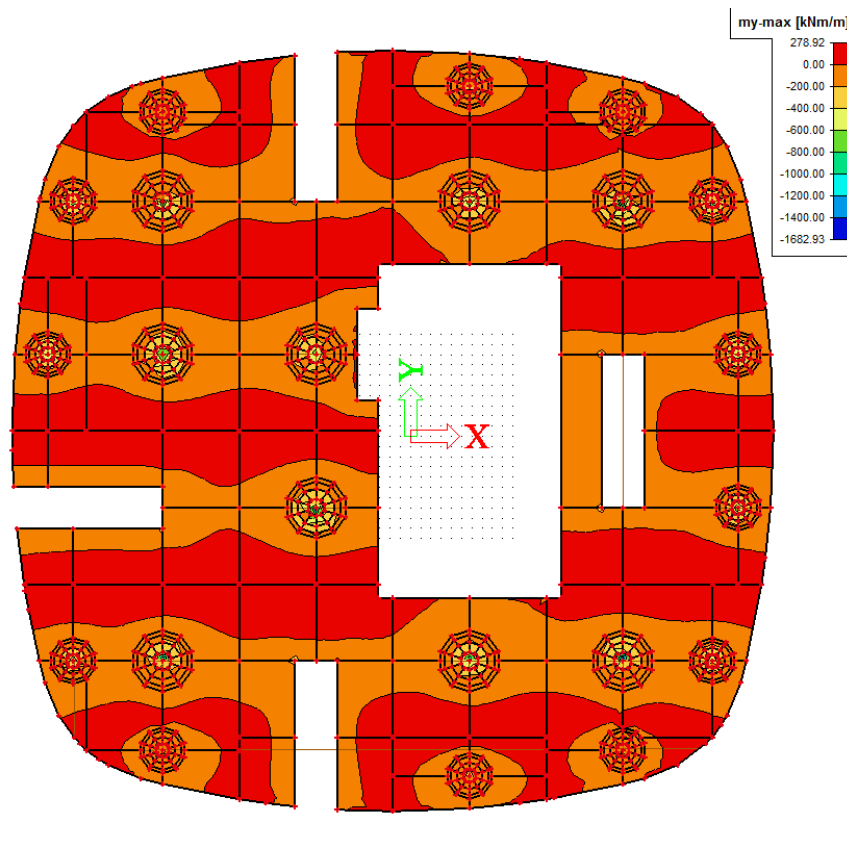


Figure 3-11  $M_y$  diagram for load pattern 1 before averaging strips

these high moments does not exist in reality due to cracking and redistribution of moments in the slab.

This was addressed by the addition of squared averaging strips around the columns. The sides of the averaging strips were calculated drawing a line inclined  $45^{\circ}$  in the edges of the column, as shown in figure 3-12. [18] Therefore the sides would be the diameter of the column plus two times the thickness of the slab. After running the calculation with the averaging strips, the peak moments decreased by 45%. (Figure 3-13 a).

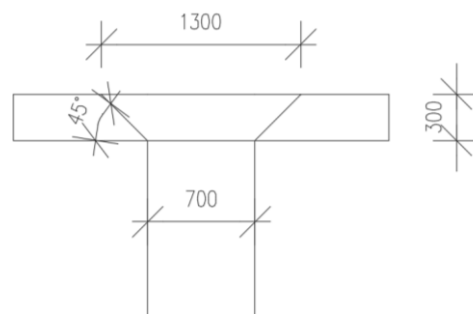
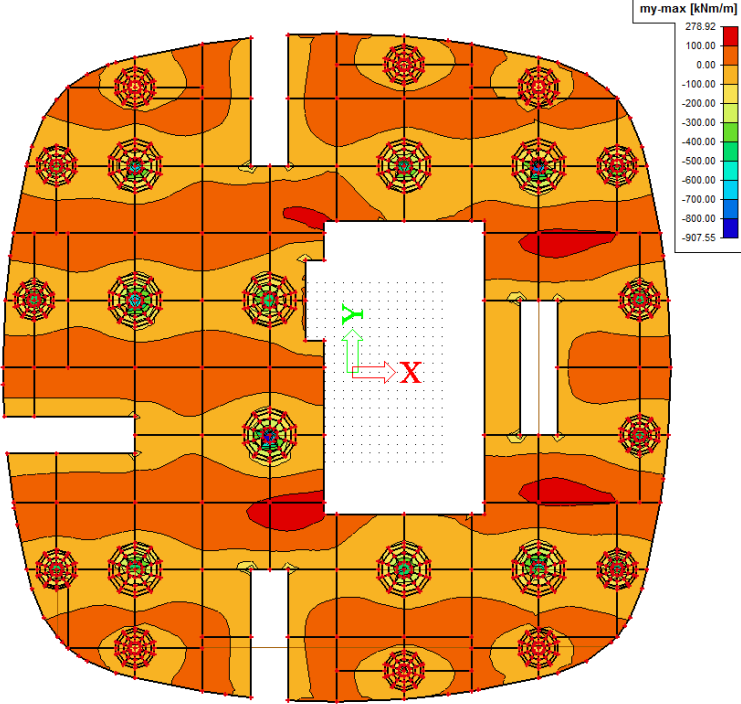


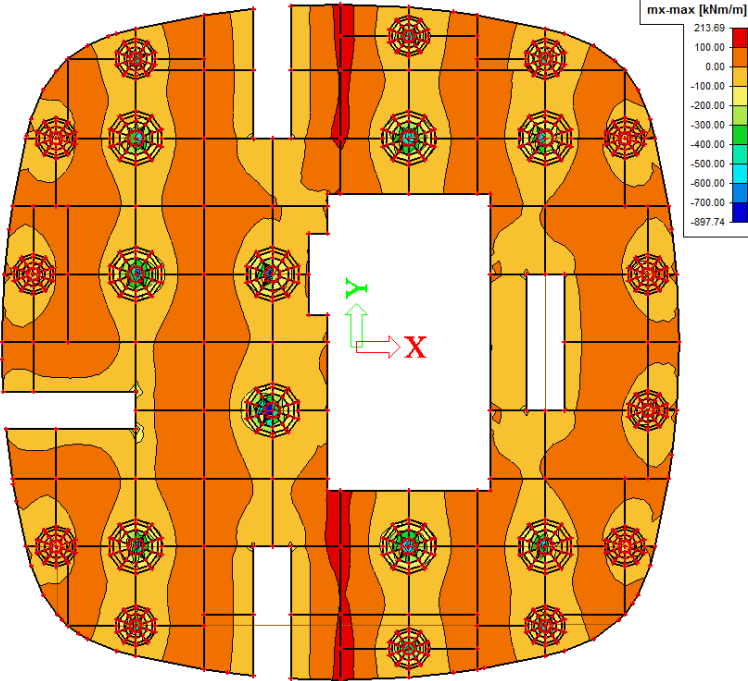
Figure 3-12 Calculation of averaging strip for 700mm diameter column

### 4.3.3.2.1. Results of analysis for dead load + load pattern I

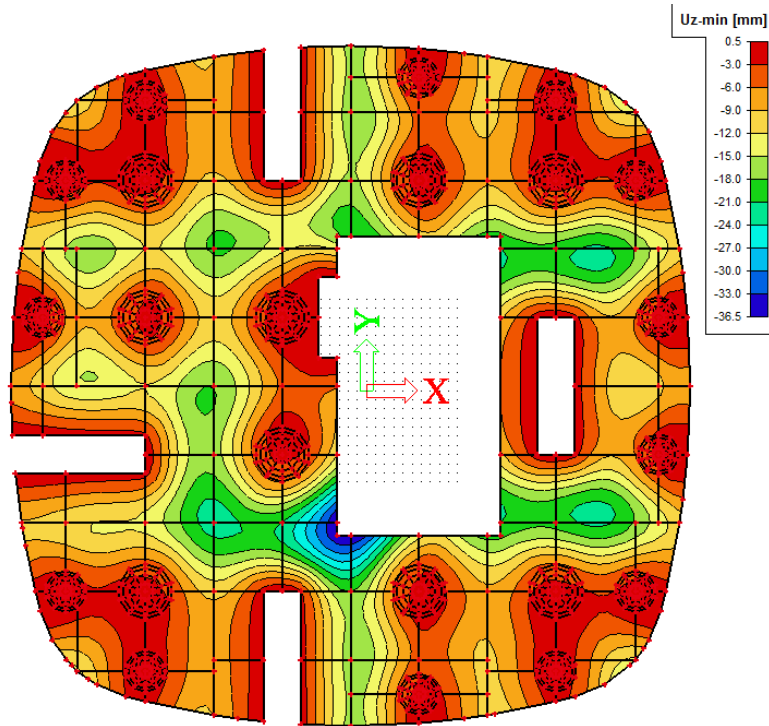
The calculation of the moment distribution and deformation of the slab for the SLS are illustrated in figures 3-13 a-c



(a) My



(b) Mx

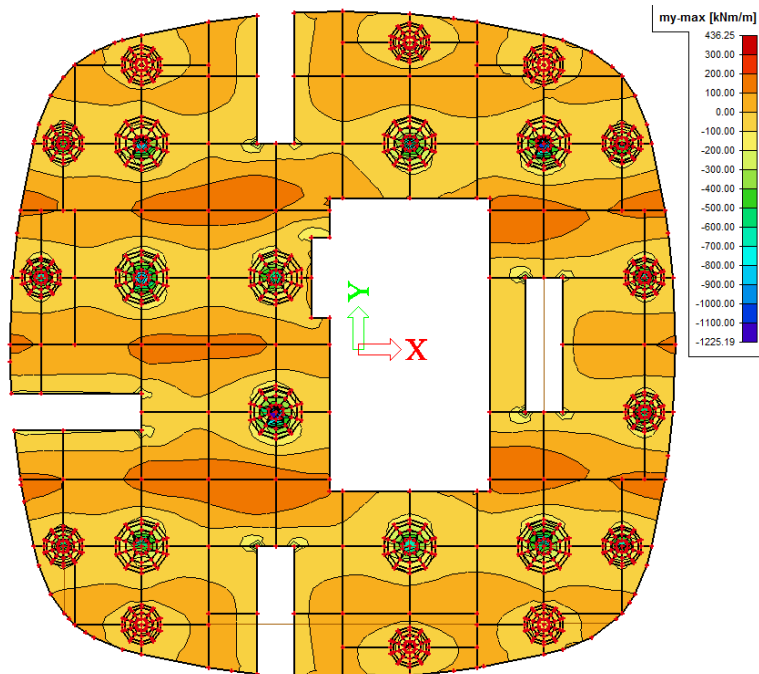


(c) Deflection

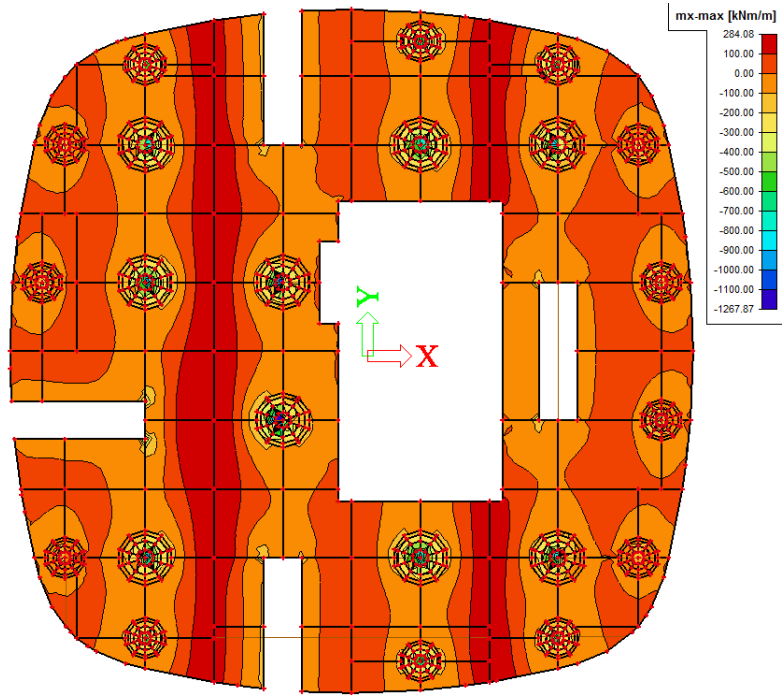
Figure 3-13 Diagrams for dead load + load pattern 1

#### 4.3.3.2.2. Results of analysis for dead load + load pattern 2

The calculation of the moment distribution and deformation of the slab for the SLS are illustrated in figures 3-14 a-c

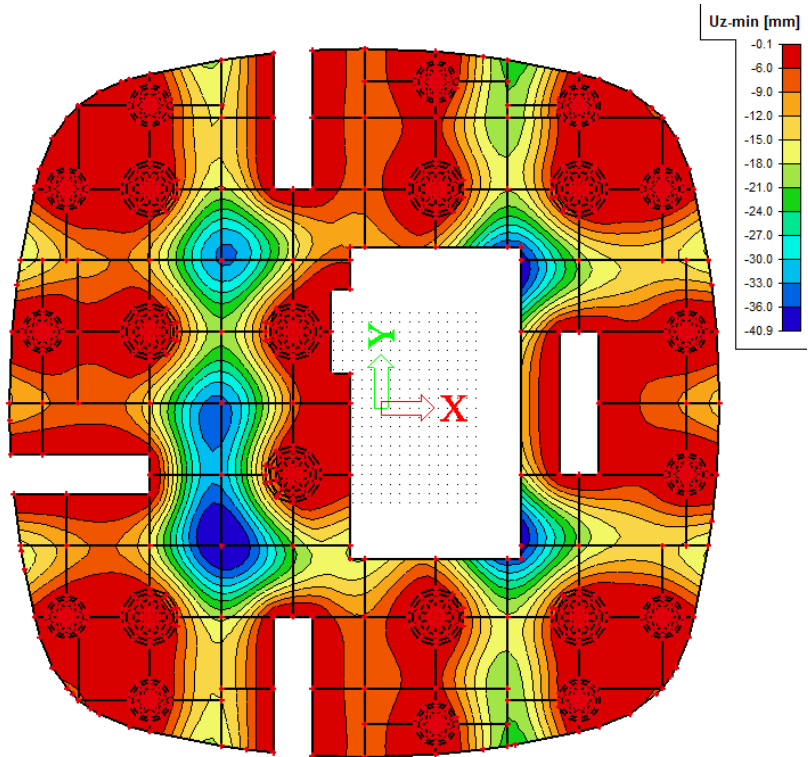


(a) My



(b) M

x

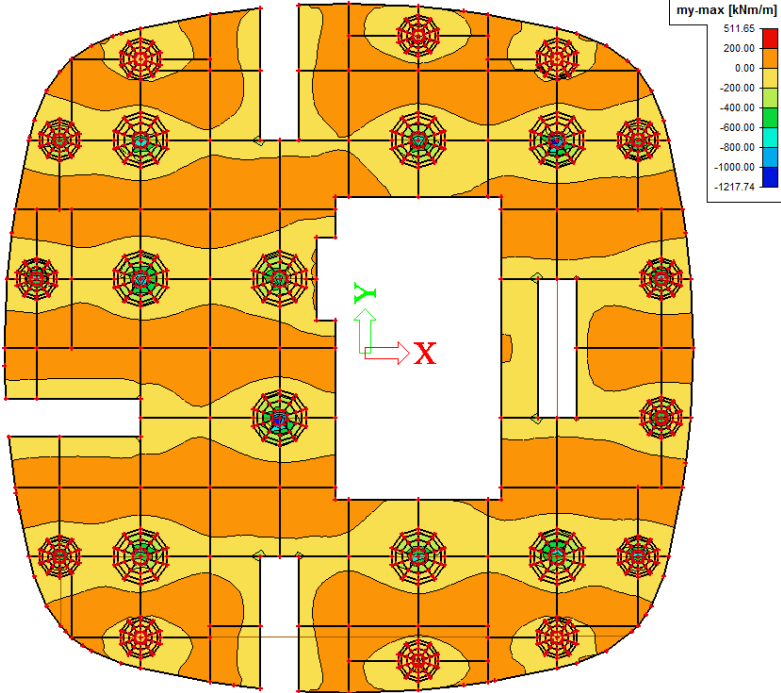


(c) Deflection

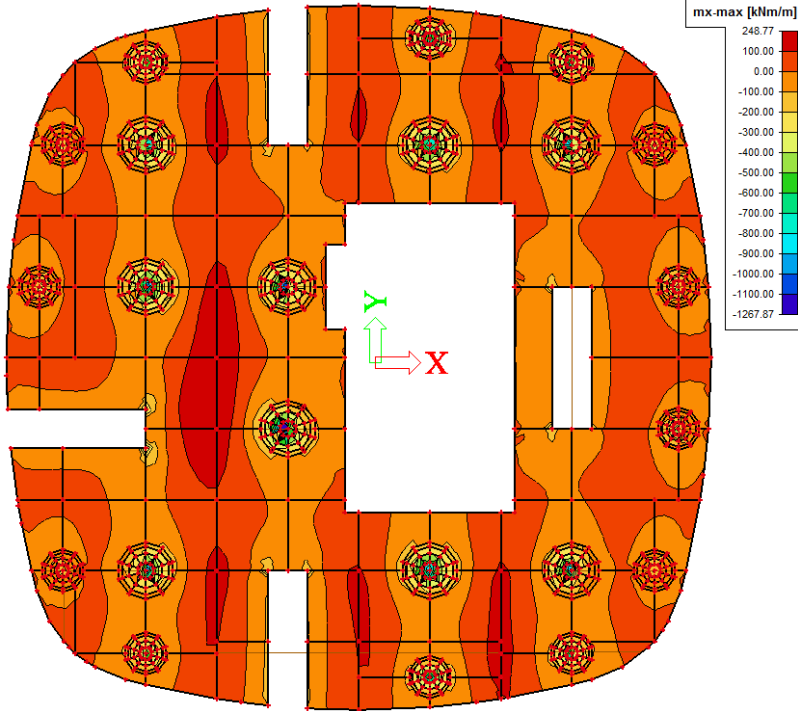
Figure 3-14 Diagrams for dead load + load pattern 2

### 4.3.3.2.3. Results of analysis for dead load + load pattern 3

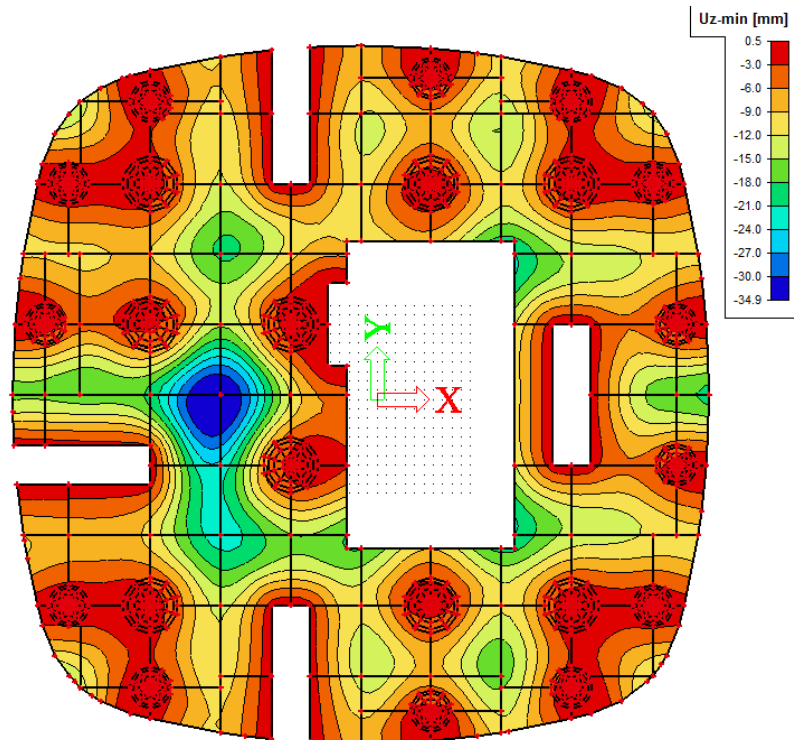
The calculation of the moment distribution and deformation of the slab for the SLS are illustrated in figures 3-15 a-c



(a) My



(b) Mx

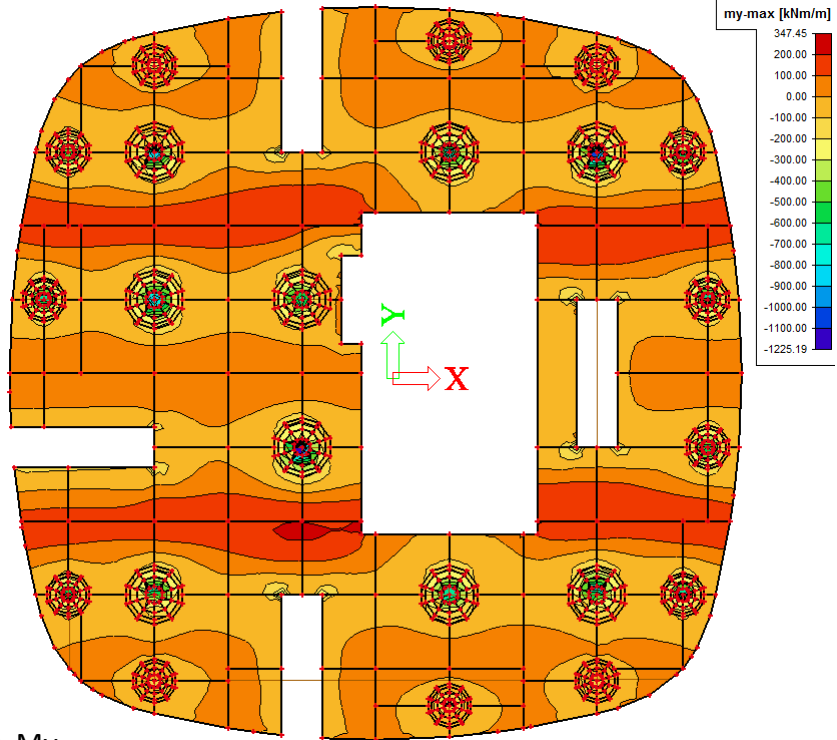


(c) Deflection

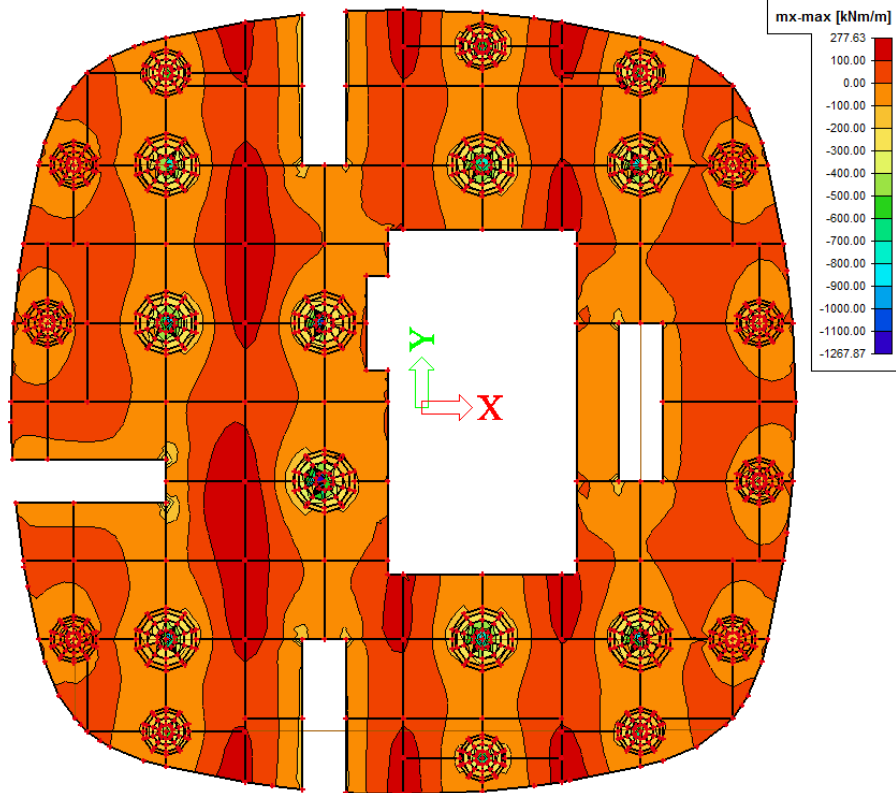
Figure 3-15 Diagrams for dead load + load pattern 3

#### 2.4. Results of analysis for dead load + load pattern 4

The calculation of the moment distribution and deformation of the slab for the SLS are illustrated in figures 3-16 a-c

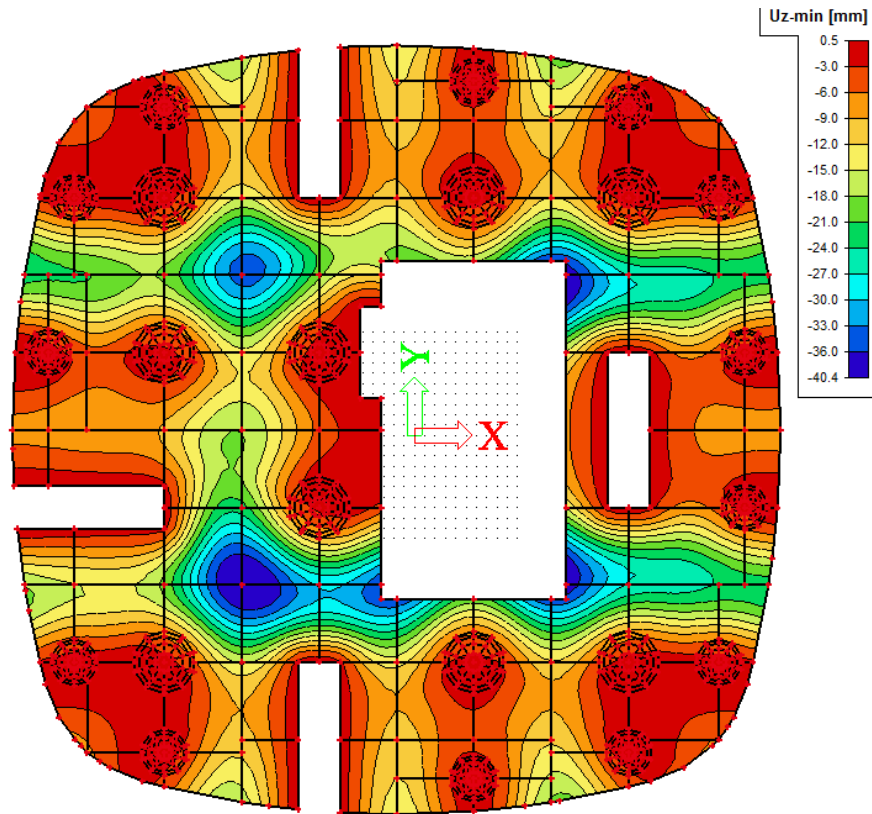


(a) My



(b) Mx



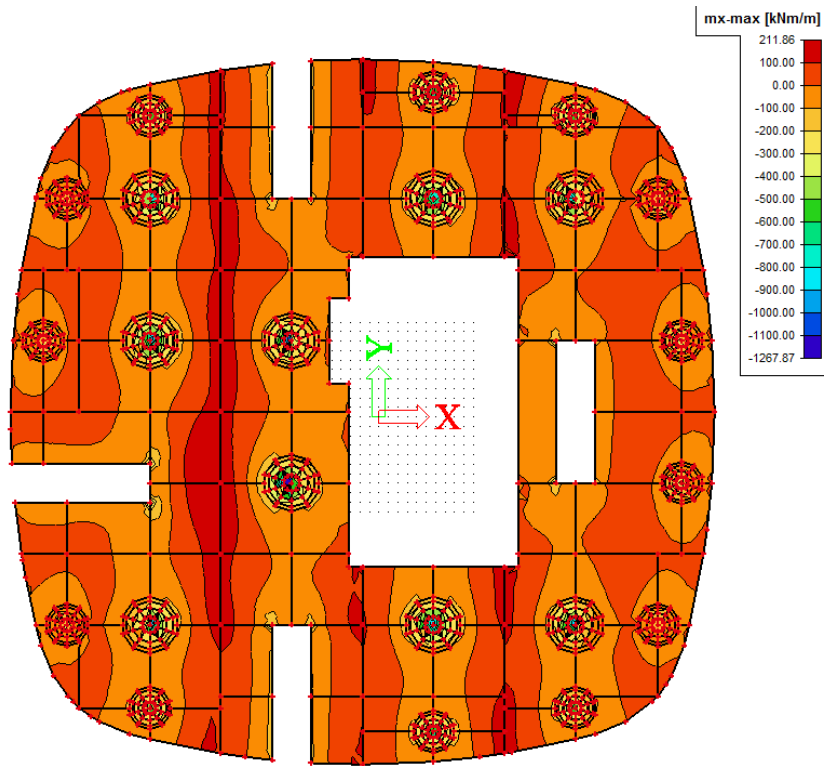


(c) Deflection

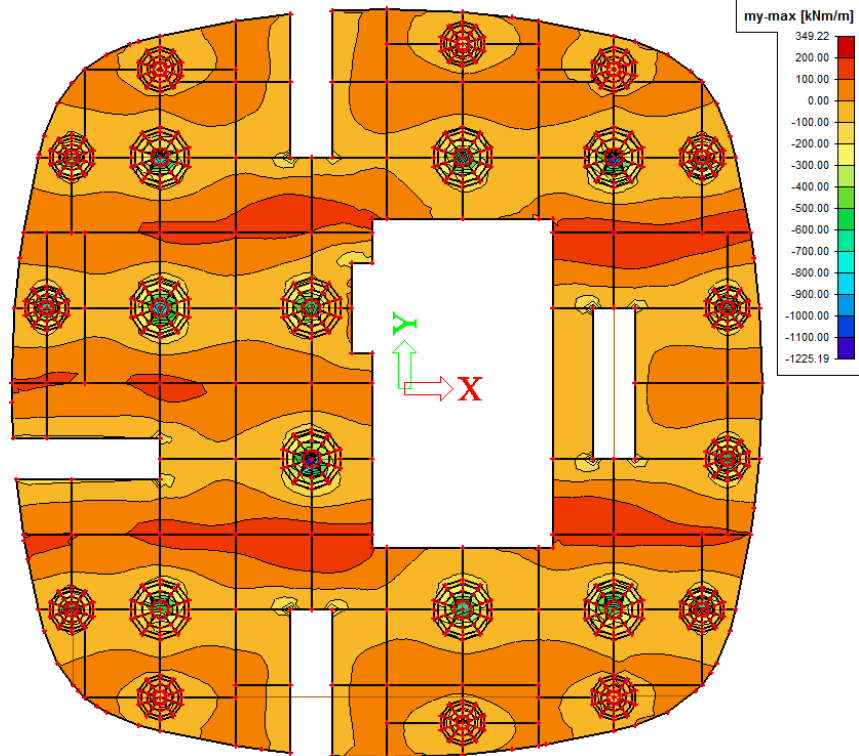
Figure 3-16 Diagrams for dead load + load pattern 4

## 2.5. Results of analysis for dead load + load pattern 4

The calculation of the moment distribution and deformation of the slab for the SLS are illustrated in figures 3-17 a-c



(a) My



(b) Mx

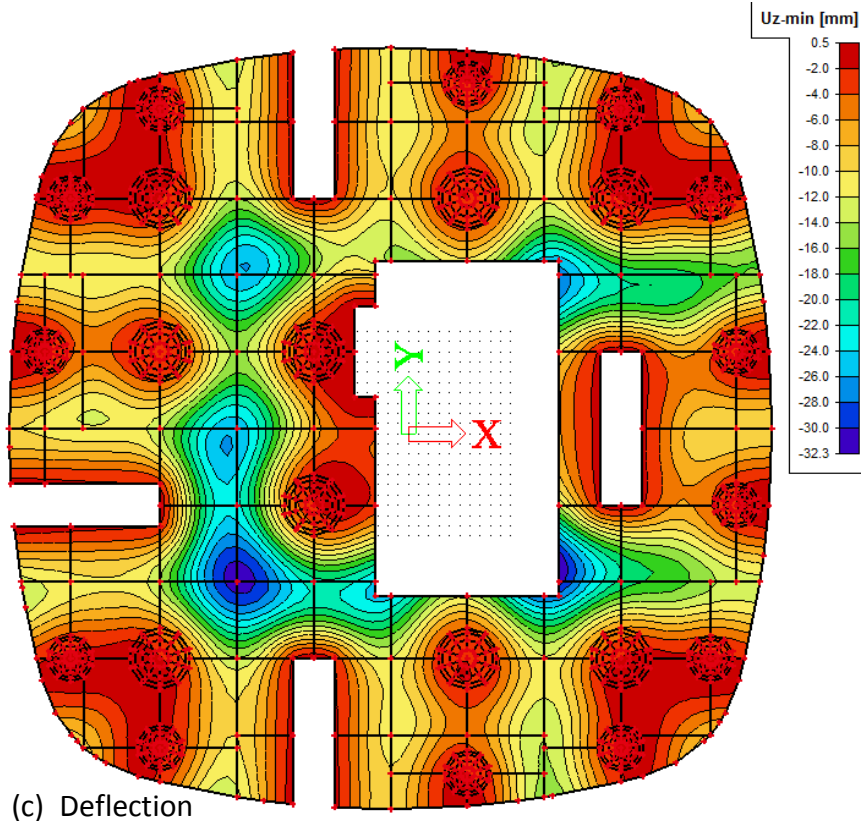


Figure 3-17 Diagrams for dead load + load pattern 5

Table 3-2 shows that a maximum deflection of 40.9 mm was computed.

Load pattern	Deflection (mm)
Load pattern 1	36.5
Load pattern 2	40.9
Load pattern 3	34.9
Load pattern 4	40.4
Load pattern 5	32.3
<b>Envelope</b>	40.9

Table 3-2 Maximum deflections of 3rd floor slab for the SLS

In addition to the immediate deflection due to live load, the long-term deformation due to the combined effects of creep and shrinkage will be considered. This additional deflection will be calculated by multiplying the immediate deflection by the factor  $\lambda_{\Delta}$  shown in Equation 3.1 and 3.2 [14]:

$$\lambda_{\Delta} = \frac{\mu\xi}{1 + 50\mu\rho'} \quad (3.1)$$

$$\mu = 1.4 - \frac{f_c'}{10000} \quad (f_c \text{ in psi}) \quad (3.2)$$

$$0.4 \leq \mu \leq 1.0$$

In which  $A_s'$  is the compression steel,  $\rho' = A_s' / bd$  and  $\xi$  is a time-dependent factor and it is related to the material properties. For simple and continuous spans the values of  $\rho'$  should be taken from the mid-span or in the support for cantilevers. For two way slabs, a five-year value of  $\xi = 3$  is specified in [14]. This factor is specified in the ACI Code.

The reinforcement will be design for the part of the slab indicated in figure # in order to determine the amount of reinforcement needed in the mid-span and therefore calculate the coefficient  $\lambda_{\Delta}$ .

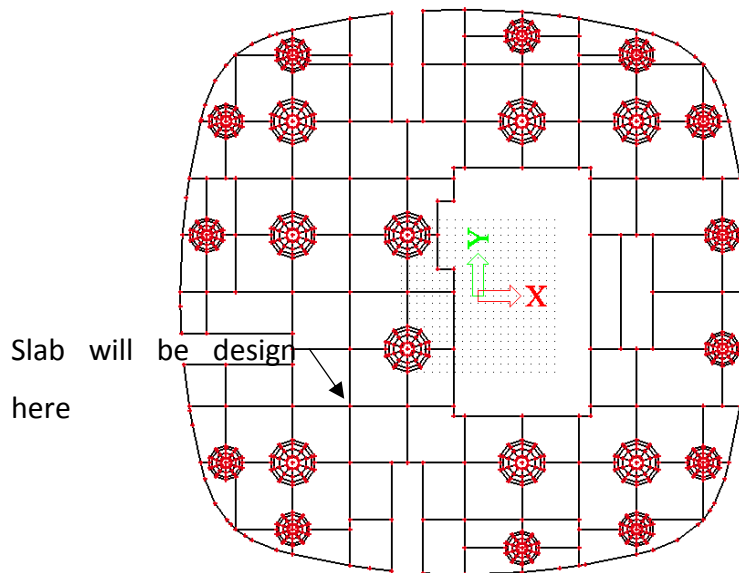


Figure 3-18 Point of slab designed

The exposure class for the library is XC1, the reinforcing steel is B500B and the concrete class C35/45. The building will be design to have a working life of 50 years.

$$f_{cd} = \frac{f_{ck}}{\gamma_c} = \frac{35}{1.5} = 23.33 \text{ Mpa}$$

$$f_{yd} = \frac{f_{yd}}{\gamma_s} = \frac{500}{1.15} = 435 \text{ MPa}$$

We will assume that the reinforcement for the mid-span is  $\phi=16\text{mm}$

$$c_{\text{nom}} = c_{\text{min}} + \Delta c_{\text{dev}}$$

$$c_{\text{min}} = \max(c_{\text{min,b}}; c_{\text{min,dur}} + \Delta c_{\text{dur},\gamma} - \Delta c_{\text{dur},\text{st}} - \Delta c_{\text{dur},\text{add}}; 10\text{mm})$$

$$c_{\text{min,b}} = 16\text{mm}$$

$c_{\text{min,dur}} \Rightarrow$  Exposure class XC1 and structural class S4, but it is a slab so we can reduce the structural class to S3.

Therefore,  $c_{\text{min,dur}} = 10 \text{ mm}$

$\Delta c_{\text{dur},\gamma}$ ,  $\Delta c_{\text{dur},\text{st}}$ ,  $\Delta c_{\text{dur},\text{add}}$  are all considered zero.

$$c_{\text{min}} = \max(16; 10; 10) = 16 \text{ mm}$$

$$\Delta c_{\text{dev}} = 10\text{mm}$$

$$c_{\text{nom}} = 16 + 10 = 26\text{mm} \approx 30\text{mm}$$

The cover is 30 mm.

In table 3-3, we can find the bending moments in the X and Y direction and the torsion moment for all the load patterns and the maximum values computed. This values were taken from the SCIA model.

Load Patterns	$m_x$ (kNm/m)	$m_y$ (kNm/m)	$m_{xy}$ (kNm/m)
Load pattern 1	85.9	89.3	29
Load pattern 2	165.8	141.2	31.6
Load pattern 3	93.5	83.4	25.3
Load pattern 4	143.4	167	31.5
Load pattern 5	118	114.4	15.88
<b>Envelope</b>	<b>165.8</b>	<b>167</b>	<b>31.6</b>

Table 3-3 Values for bending moment and torsion

With these values we can calculate the required resisting bending moments at both surfaces.

$$m_{Rdx} = -m_x + |m_{xy}| = -165.8 + 31.6 = -134.2 \text{ kNm/m} < 0$$

$$d_x = h - c - \phi/2 = 300 - 30 - 10/2 = 265 \text{ mm}$$

$$z = 0.85d = 225.3 \text{ mm}$$

$$a_{s,\min} = 0.0013 * b * d = 0.0013 * 265 * 1000 = 344.5 \text{ mm}^2/\text{m}$$

$$a_{s,\max} = 0.04 * b * h = 0.04 * 300 * 1000 = 12000 \text{ mm}^2/\text{m}$$

Does not require any reinforcement. A basic reinforcement of  $\phi 10$  every 150mm will be used.

$$a_{s,\text{prov}} = 524 \text{ mm}^2$$

$$x = \frac{a_{s,\text{prov}} * f_{yd}}{0.8 * f_{cd} * b} = \frac{335 * 435}{0.8 * 23.3 * 1000} = 12.2 \text{ mm}$$

$$\xi = \frac{x}{d} = 0.05 < 0.45$$

In table Table 3-4 Design of conventional reinforcement for slab, we can see the summary of the results in both directions for the design of the slab in the indicated area. We can see that the reinforcement on the top is 524 mm<sup>2</sup>/m. This value is replaced in Equation 3.1 and 3.2 together with the value of 35Mpa in psi which is 5076 psi.

$$\rho' = \frac{A'_s}{b \cdot d} = \frac{524}{1000 * 265} = 0.00198$$

$$\mu = 1.4 - \frac{5076}{10000} = 0.89$$

$$\lambda_{\Delta} = \frac{\mu \xi}{1 + 50 \mu \rho'} = \frac{0.89 * 3}{1 + 50 * 0.89 * 0.00198} = 2.45$$

$$\Delta_t = \lambda_{\Delta} * \Delta = 40.9 * 2.45 = 100.21 \text{ mm}$$

The additional deflection would be of the order of 100.21 mm. From the Eurocode we can determine a tolerance for the deflection of the span divided by 250. In this case, 15000/250=60mm. We can conclude that the deflection of the slab using conventional reinforced concrete surpasses the tolerance and, therefore, it demonstrate the need to use pre-stressed concrete in our structure.

mx	my	mxy	Surface	direction	torque moment	d	z (0,85d)	a <sub>s,req</sub>	Reinforcement				a <sub>s,prov</sub>		x	ξ	mRd	Check			
[kNm/m]					[kNm/m]	[mm]	[mm]	[mm <sup>2</sup> /m]	∅		á	mm	[mm <sup>2</sup> /m]		[mm]	[-]	[kNm/m]				
165.80	167.00	31.60	sup	H	x	-134.200	265.0	225.3	---	∅	10	á	150 mm	524	OK	12.2	0.05	OK	59.246	0.00	OK
				H	y	-135.400	255.0	216.8	---	∅	10	á	150 mm	524	OK	12.2	0.05	OK	56.969	0.00	OK
			inf	D	x	197.400	262.0	222.7	2037.7	∅	16	á	100 mm	2011	OK	46.85	0.18	OK	212.758	0.93	OK
				D	y	198.600	246.0	209.1	2183.4	∅	16	á	100 mm	2011	OK	46.85	0.19	OK	198.764	1.00	OK

Table 3-4 Design of conventional reinforcement for slab

## 4. Reinforcement with pre-stressed concrete

### 2.1. The load balancing method

For the calculation of the pre-stressing we will use the load balancing method. This method gives us the possibility to obtain the distribution of internal forces due to the pre-stressing and to demonstrate how the pre-stressing is capable of changing this distribution. The tendon affects the structure by the concentrated force at the anchoring and through the forces in points where the direction of the tendon changes. As shown in Figure 4-1, when the applied force P changes its direction and the force acts under a different angle at the right side and the left side of a determined point, a resultant force  $r(x)$  is created. The sum of the vertical and horizontal components of all the forces R along the beam then create what we can call the equivalent load (Figure 4-3). The angular change along the length of the tendon is usually very

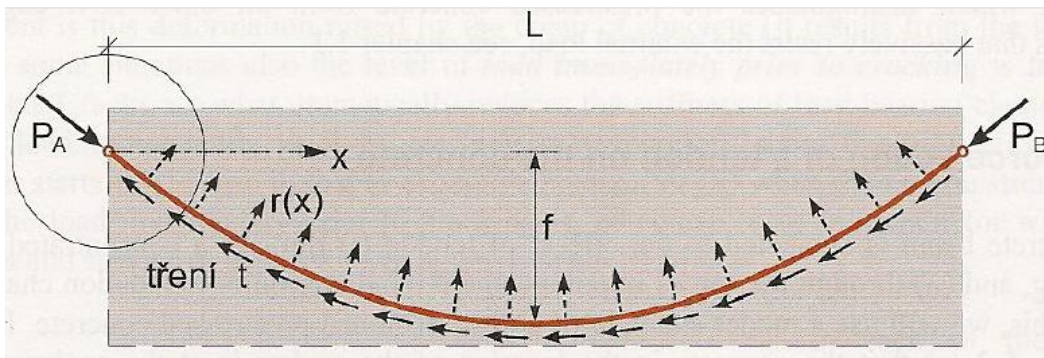


Figure 4-1 Real force action of tendon on concrete

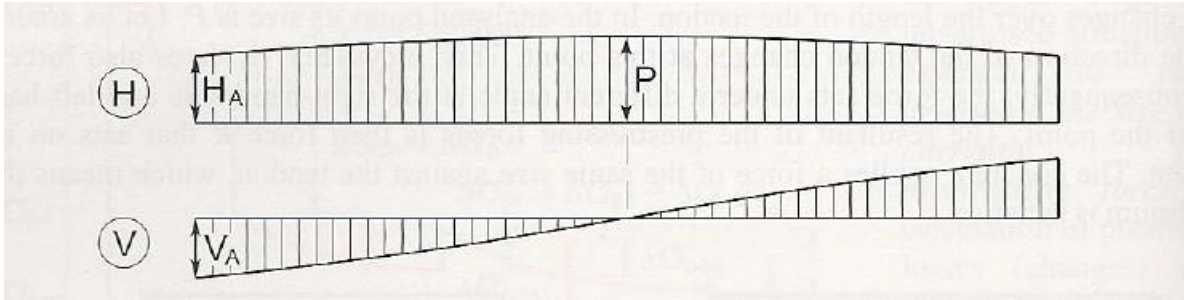


Figure 4-3 Distribution of horizontal and vertical components of pre-stressing force when  $P=const$

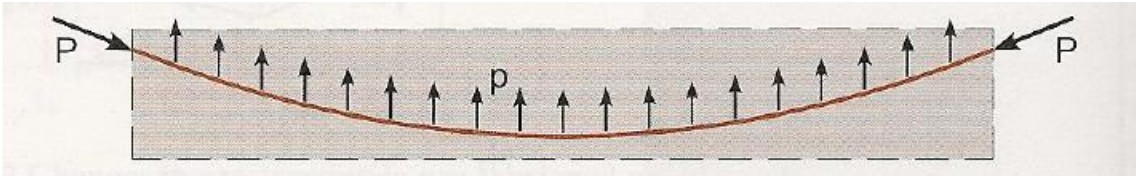


Figure 4-2 Equivalent load

small, so the horizontal force is practically constant and the radial force can be considered as a uniformly distributed vertical load. This assumption can be done when the ratio between the camber  $f$  and the span  $L$  is lower than  $1/15$ . (Figure 4-2)

To calculate the vertical distributed load  $p$  we can use the Equation 4.1, in which  $H$  is the pre-stressing force,  $L$  is the span and  $f$  is the camber. We can calculate  $p$  in order to fully or partially balance the self-weight and the live load. It is recommended a balancing of 80 to 100% of the permanent loads. In the case of our structure, 80% of the permanent loads will be balanced. [19]

$$p = H \frac{8f}{L^2} \quad (4.1)$$

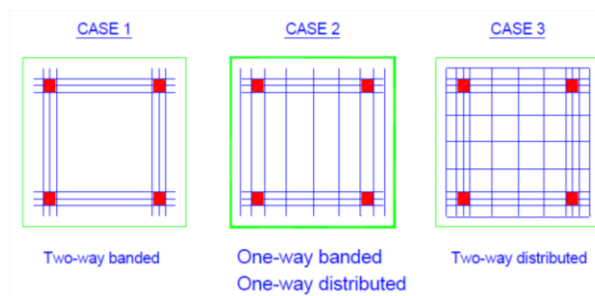


Figure 4-4 Types of pre-stressing layout



## 2.2. Detailing

The laying out of the pre-stressing tendons can be done in different ways, some of them are shown in Figure 4-4 . Is important to know that the tendons inside of the span transfer the load to the column strips. The tendons in the column strips transfer this load into the columns and edge beams. (Figure 4-5) The tendons inside of the span can be partially or fully substituted by conventional reinforcement. [19] For this slab, it was decided to use the case 1 and to reinforce the mid-span with conventional concrete.

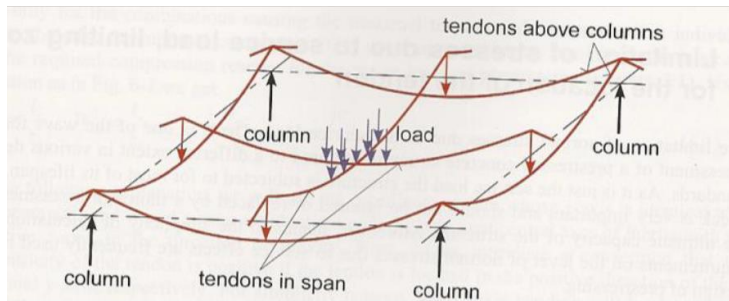


Figure 4-5 Distribution of loads in a flat slab

## 2.3. Tendon properties

The type of tendon is a 4-strand tendon in a Flat Multiplane Anchorage FMA from the company DYWIDAG and a flat plastic duct (Figure 4-6). This tendon is designed to be installed in thin members such as top slabs of box-girder bridges and pre-stressed flat slabs. The strands will be Y1770S7 and the specifications are shown in *Error! No se encuentra el origen de la referencia.* and Figure 4-9.



Figure 4-6 Flat Multiplane Anchorage (DYWIDAG)

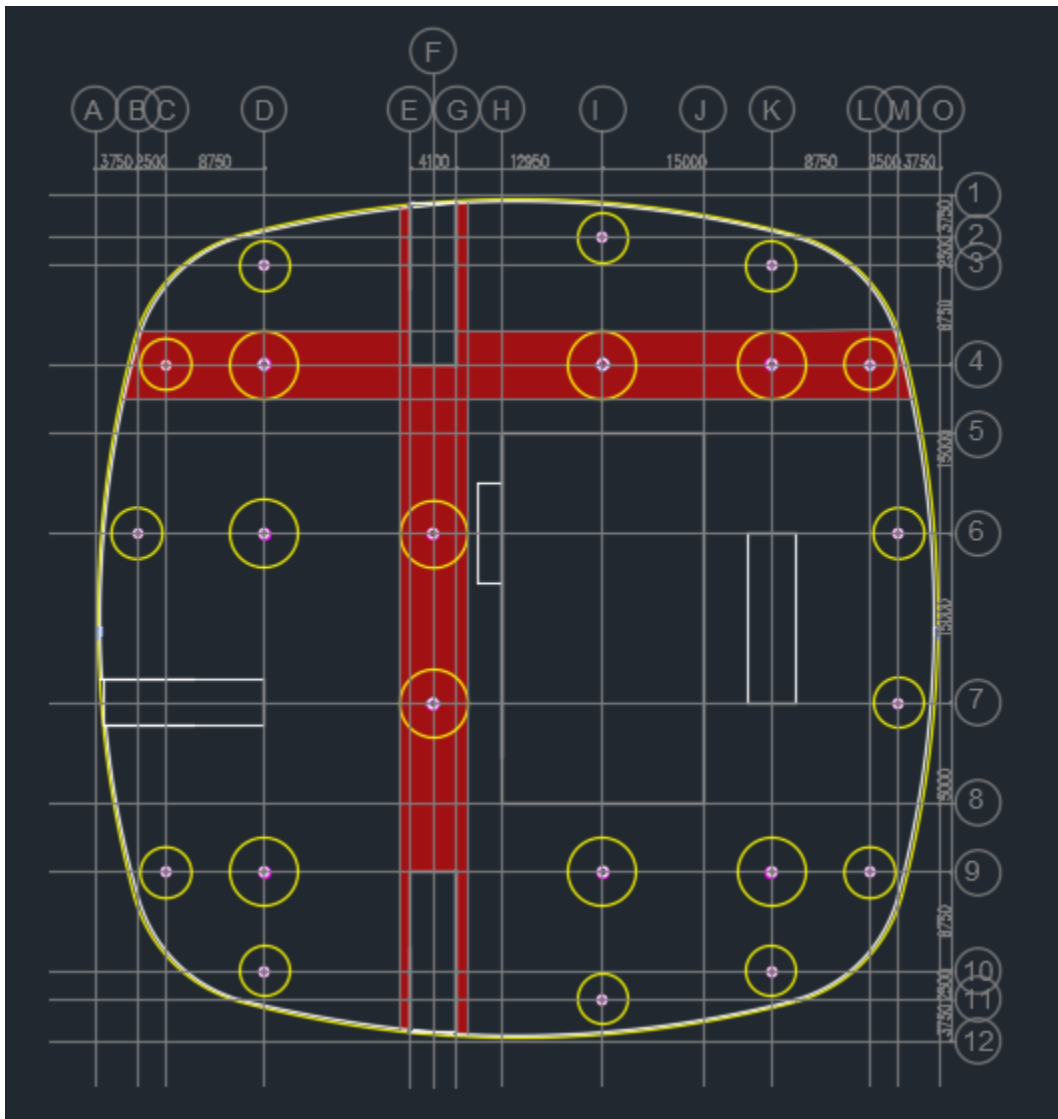


Figure 4-7 Plan of analyzed slab

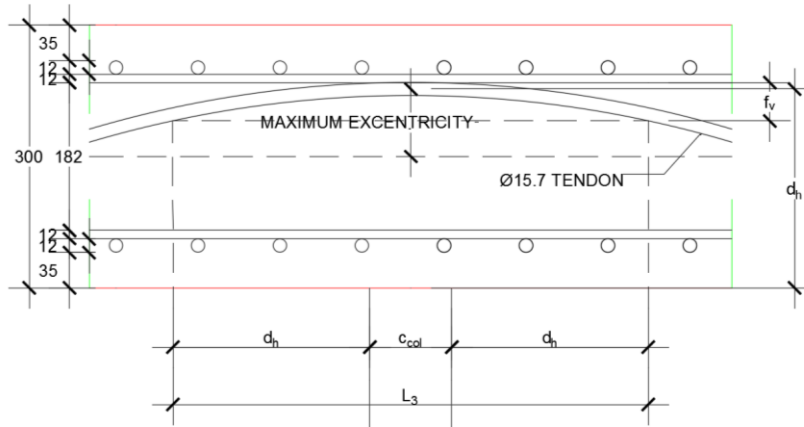


Figure 4-8 Detail of slab section

Nominal diameter		Designation according to prEN 10138-3 <sup>5</sup>	Nominal tensile strength
mm	inch	—	N/mm <sup>2</sup>
15.3	0.6	Y1770S7	1 770
15.3	0.6	Y1860S7	1 860
15.7	0.62	Y1770S7	1 770
15.7	0.62	Y1860S7	1 860

Figure 4-9 Tensile strength for 7-wire strand

#### 2.4. Loss of pre-stressing due to friction and wobble

At the moment of the pre-stressing, the cable will be in contact with the duct causing loss of pre-stress. Similarly, because the duct can never be held rigidly in place, there is a certain amount of deviation (wobble) from the intended profile. This effects can be calculated with Equation 4.2.  $P_1$  is the pre-stressing force in the jacking end,  $P_2$  is the force in the anchored end,  $\mu$  is the friction coefficient of the duct,  $\theta$  is the sum, in radians, of angular displacements throughout the tendon irrespective of the sign over the length  $x$  and  $k$  is a constant called the wobble coefficient in the range  $0.005 < k < 0.01$ .

$$P_1 = P_2 e^{-\mu(\theta+kx)} \quad (4.2)$$

From Anex 2 we can take the values for  $k$  and  $\mu$  as 0.2 and 0.08 l/m.

Strand			Y1770S7		Y1860S7	
			15.3	15.7	15.3	15.7
Characteristic tensile strength	$R_m$	N/mm <sup>2</sup>	1 770		1 860	
Nominal diameter of strand	$d$	mm	15.3	15.7	15.3	15.7
Nominal diameter of outer wire	$d_o$	mm	5.0	5.2	5.0	5.2
Diameter of core wire $d$	$d'$	mm	$\geq 1.03 \cdot d_o$			
Nominal mass per metre	$M$	g/m	1 093	1 172	1 093	1 172
Nominal cross sectional area	$A_p$	mm <sup>2</sup>	140	150	140	150
Characteristic value of maximum force	$F_m$	kN	248	266	260	279
Maximum value of maximum force	$F_{m, max}$	kN	285	306	299	321
Characteristic value of 0.1% proof force <sup>1)</sup>	$F_{p0.1}$	kN	218	234	229	246
Minimum elongation at maximum force, $L_0 \geq 500$ mm	$A_{gt}$	%	3.5			
Modulus of elasticity	$E$	N/mm <sup>2</sup>	195 000 <sup>2)</sup>			
Relaxation after 1 000 h, for an initial force of	—	%	$\leq 2.5$			
	—	%	$\leq 4.5$			

NOTE

- 1) For strands according to prEN 10138-3, 09.2000, the value shall be multiplied by 0.98
- 2) Standard value

Figure 4-10 Specifications for 7-wire strands

To calculate the angular displacements we will assume a three-parabola tendon profile (Figure 4-11) at the end spans and a four parabola profile (Figure 4-12) in the middle spans. For the three tendon parabola,  $a = c = 0.1L$ . The relation between  $a$ ,  $b$  and  $c$  can be express with Equations 4.3-4.7. To calculate the curvature at B and D the equation 4.8 and 4.9 will be used. For the four-parabola profile,  $b$  has the length of half of the span because the eccentricity at

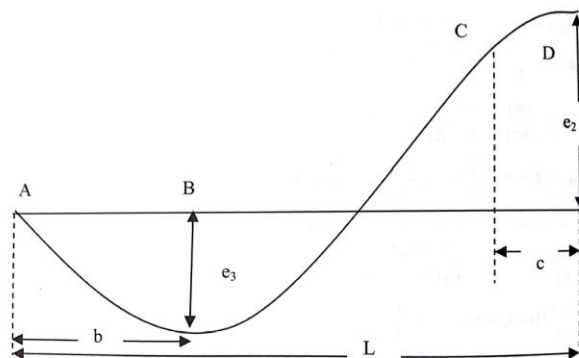


Figure 4-11 Three parabola profile

the interior supports is constant and, therefore, the profile is symmetric. The rotation in B and D have the same value as well because of this. [9]

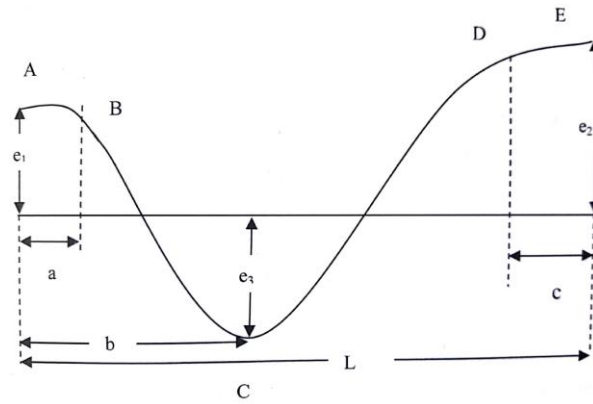


Figure 4-12 Four parabola profile

$$\frac{b}{L} = \frac{b - \sqrt{B^2 - 4AC}}{2A} \quad (4.3)$$

$$A = 1 - \alpha \quad (4.4)$$

$$B = \left(2 - \alpha \frac{a}{L} - \frac{c}{L}\right) \quad (4.5)$$

$$\alpha = \frac{(e_2 + e_3)}{(e_1 + e_3)} \quad (4.6)$$

$$C = \left(1 - \frac{c}{L}\right) \quad (4.7)$$

$$\theta_B = \frac{2(e_1 + e_3)}{b} \quad (4.8)$$

$$\theta_D = \frac{2(e_2 + e_3)}{L - b} \quad (4.9)$$

## 2.5. Anchorage set loss

After the concrete has cured and obtained the necessary strength, the wedges are inserted inside the anchor casting and the strand is stressed. When the jack releases the strand, it retracts slightly and pulls the wedges into the anchor. This slip is known as the draw-in of the wedges and it is of the order of 6-8 mm. The draw-in only occurs in a part of the length of the strand that can be calculated with Equation 4.10, in which  $p$  is the loss of pre-stress due to friction per length unit. It is assumed that the bonded length in a tendon is longer than the length  $l$  but, in small tendons, the draw-in occurs in the whole length. The loss of pre-stressing would be expressed as  $2pl$ . [9]

$$l = \sqrt{\frac{\Delta A_{ps} E_s}{p}} \quad (4.10)$$

## 2.6. Calculation of number of tendons

The calculation for the axis F will be shown as an example.

### Prestressing steel

$$f_{pk} = 1770 \text{ MPa}$$

$$f_{p0,1k} = 1570 \text{ MPa}$$

$$\text{For four tendons } A_p = 4 \cdot 150 = 600 \text{ mm}^2$$

$$\sigma_{p,max} = \text{Min}(0.8 \cdot f_{pk}, 0.9 \cdot f_{p0,1k}) = 1413 \text{ MPa}$$

The  $\sigma_{p,max}$  will be set at 1410 MPa

$$P_{max} = \sigma_{max} \cdot A_p = 1410 \cdot 0.0006 = 846 \text{ KN}$$

The maximal force per 4-strand tendon during tensioning is 846KN.

$E_s = 195 \text{ GPa}$

### Loads

$$g_{0,k} = 25 * h = 7.5 \text{ KN/m}^2$$

$$g_{1,k} = 1 \text{ KN/m}^2$$

$$g_k = 7.5 \text{ KN/m}^2$$

$$\text{Load to balance} = (g_{0,k} + g_{1,k}) * 0.8 = 6.8 \text{ KN/m}^2$$

The slab will be divided into column and middle strips as shown in Figure 4-7. The column strip would have the width of the span divided by 2 should no column drop panel would be there. In this case, we have column capital (6 m) which are wider than the span divided by 3 ( $15/3=5 \text{ m}$ ), so we will consider the width of the column strip the same as the capitals.

$$\text{Load for one strip: } q = 6.8 * 6 = 40.8 \text{ KN/m}$$

### Calculation of eccentricity

A cover of  $c_d=35 \text{ mm}$  is assumed.

Mild reinforcement:  $\phi = 12 \text{ mm}$

Centre of strand located at:  $c_d + 2 * \phi + 0.5 * 15.7 = 66.85 \text{ mm}$  (Figure 4-6)

Maximum excentricity:  $d * 0.5 - 66.85 = 83.15 \text{ mm}$ . Assumed an excentricity of 0 mm at end spans

## **2.5.1. Results for axis F**

### **Loss due to friction in span 4-5**

Jacking force  $P_4 = 846 \text{ KN}$ . The tendon will be stressed from one end.

$$e_1 = 0$$

$$e_2 = 83.15 \text{ mm}$$

$$e_3 = 83.15 \text{ mm}$$

$$a = c = 0.1 * L = 1500 \text{ mm}$$

$$\alpha = \frac{e_2 + e_3}{e_1 + e_3} = 2$$

$$A = 1 - \alpha = -1$$

$$B = 2 - \alpha \frac{a}{L} - \frac{c}{L} = 1.7$$

$$C = \left(1 - \frac{c}{L}\right) = 0.9$$

$$\frac{b}{L} = \frac{b - \sqrt{B^2 - 4AC}}{2A} = 0.423$$

$$b = 6356.6 \text{ mm}$$

$$L - b = 8643.4 \text{ mm}$$

Replacing in equation 4.8 and 4.9:  $\theta_B = 0.0262 \text{ rad}$ ,  $\theta_D = 0.0385 \text{ rad}$

$$\theta = \theta_B + 2\theta_D = 0.1031 \text{ rad}$$

$$\mu(\theta + kL) = 0.0446$$

Replacing in equation 4.2:  $P_3 = P_4 e^{-\mu(\theta + kx)} = 809 \text{ kN}$

### Loss due to friction in span 5-6

This is a middle span, therefore it is symmetrical

$$e_1 = 83.15$$

$$e_2 = 83.15$$

$$e_3 = 83.15$$

$$a = c = 0.1L = 1500 \text{ mm}$$

$$b = 0.5L = 7500 \text{ mm}$$

Replacing in equation 4.8:  $\theta_B = \theta_D = 0.0443 \text{ rad}$

$$\theta = 2(\theta_B + \theta_D) = 0.1774 \text{ rad}$$

Replacing in equation 4.2:  $P_6 = P_5 e^{-\mu(\theta + kx)} = 762 \text{ kN}$



### Loss due to friction in span 6-7

This span is simetrical to the span 4-5 and it has the same length. Thus, it has the same angular change as the first span and  $\mu(\theta+kL)$  has the same value too:

$$\mu(\theta+kL) = 0.05$$

$$P_7 = P_6 e^{-\mu(\theta+kx)} = 729 \text{ kN}$$

The force in point 7 after stressing is 729 kN.

The summary of the calculated values are shown in Table 4-3

<b>Span</b>	4-5	5-6	6-7
<b>L (mm)</b>	15000	15000	15000
<b>e<sub>1</sub> (mm)</b>	0	83.15	83.15
<b>e<sub>2</sub> (mm)</b>	83.15	83.15	0
<b>e<sub>3</sub> (mm)</b>	83.15	83.15	83.15
<b>a (mm)</b>	1500	1500	1500
<b>c (mm)</b>	1500	1500	1500
<b>α</b>	2		0.5
<b>A</b>	-1		0.5
<b>B</b>	1.7		1.85
<b>C</b>	0.9		0.9
<b>b/L</b>	0.4238		0.5762
<b>b (mm)</b>	6356.6	7500.0	8643.4
<b>L-b (mm)</b>	8643.4	7500.0	6356.6
<b>θ<sub>B</sub> (rad)</b>	0.0262	0.0443	0.0385
<b>θ<sub>D</sub> (rad)</b>	0.0385	0.0443	0.0262
<b>θ (rad)</b>	0.1031	0.1774	0.1031
<b>μ(θ+kx)</b>	0.0446	0.0595	0.0446
<b>Pe<sup>-μ(θ+kx)</sup> (kN)</b>	809	762	729

Table 4-1 Calculation of friction loss in axis F

### Anchorage set loss

From Anex 2 we consider the draw-in  $\Delta = 6 \text{ mm}$ .

We calculate the loss of pre-stress due to friction per length unit:

$$\frac{P_4 - P_7}{L_{total}} = \frac{841.10 - 724.87}{45} = 2.58 \text{ kN/m}$$

With equation 4.10 we calculate the length  $l$

$$l = \sqrt{\frac{6 \times 10^{-3} \times 195 \times 600}{2.58}} = 16.49 \text{ m}$$

Loss of force at anchorage:  $2pl = 85.17 \text{ kN}$

The force after anchorage in point 4 is  $P_4 = 841.1 - 85.17 = 755.93 \text{ kN}$

**Determination of number of tendons**

For the design, in the span 4-5 the force will be considered:  $\frac{P_4 + P_5}{2} = 780.17 \text{ kN}$

We will consider a loss of 15% for long-term losses:  $0.85 \times 780.17 = 663.14 \text{ kN}$

Drape on end spans:  $e_3 + \frac{(e_1 + e_2)}{2} = 83.15 + \frac{(0 + 83.15)}{2} = 124.73 \text{ mm}$

Drape on middle span:  $83.15 + \frac{(83.15 + 83.15)}{2} = 166.3 \text{ mm}$

From equation 4.1, the total pre-stressing force required:  $P = \frac{40.8 \times 15^2}{8 \times 124.73} = 9200 \text{ kN}$

Number of tendons:  $\frac{9200}{667} \approx 14$

In Table 4-4 we can see the summary of the results for the axis F

Span	4-6	6-7	7-9
<b>Force per tendon (kN)</b>	785	786	746
<b>Force after long-term losses (kN)</b>	667	668	634
<b>Drape (mm)</b>	124.73	166.30	124.73
<b>P (kN)</b>	9200	6900	9200
<b>Tendons needed</b>	14	10	15

Table 4-2 Determination of number of tendons for axis F

The result indicates that the total loss is  $(\frac{846-634}{846}) * 100 \approx 25\%$ .

In the same way, the required pre-stressing in the other axes were calculated. The pre-stressing of the outer spans was not calculated in this thesis.

In order to simplify the modeling of the pre-stressing later, instead of using the maximum eccentricity for every span, the values of the eccentricities were modified until we reached a more even number of tendons between consecutive spans. This is necessary since the spans are inconstant and it would be complicated to model every span with different number of tendons in each. Therefore, for axis F we changed the eccentricity for the middle span to have 14 tendons in every span (Table 4-5). This seems uneconomical but for the purpose of this thesis will be applied.

<b>Span</b>	4-6	6-7	7-9
<b>L (mm)</b>	15000	15000	15000
<b>e<sub>1</sub> (mm)</b>	0	83.15	83.15
<b>e<sub>2</sub> (mm)</b>	83.15	83.15	0
<b>e<sub>3</sub> (mm)</b>	83.15	40	83.15
<b>a (mm)</b>	1500	1500	1500
<b>c (mm)</b>	1500	1500	1500
<b>α</b>	2		0.5
<b>A</b>	-1		0.5
<b>B</b>	1.7		1.85
<b>C</b>	0.9		0.9
<b>b/L</b>	0.4238		0.5762
<b>b (mm)</b>	6356.6		7500.0
<b>L-b (mm)</b>	8643.4	7500.0	6356.6
<b>θ<sub>B</sub> (rad)</b>	0.0262	0.0328	0.0385
<b>θ<sub>D</sub> (rad)</b>	0.0385	0.0328	0.0262
<b>θ (rad)</b>	0.1031	0.1314	0.1031
<b>μ(θ+kx)</b>	0.0446	0.0503	0.0446
<b>Pe<sup>-μ(θ+kx)</sup> (kN)</b>	809	769	736
<b>Draw in (mm)</b>	6		
<b>Loss per unit (kN/m)</b>	2.45		
<b>l (m)</b>	16.93		
<b>2pl (kN)</b>	83		
<b>Force at anchorage (kN)</b>	763		
<b>Span</b>	4-6	6-7	7-9
<b>Force per tendon (kN)</b>	786	789	753
<b>Force after long-term losses (kN)</b>	668	671	640
<b>Drape (mm)</b>	124.73	123.15	124.73
<b>P (kN)</b>	9200	9318	9200
<b>Tendons needed</b>	14	14	14

Table 4-3 Summary of determination of number of tendons for axis F

## 2.5.2. Results for axis H

In Table 4-6, the results for the axis H are shown. The result indicates that the total loss is

$$\left(\frac{846-641}{846}\right)*100 \approx 25\%.$$

<b>Span</b>	1-2	2-4	4-5
<b>L (mm)</b>	3100	11250	6150
<b>e<sub>1</sub> (mm)</b>	0	83.15	83.15
<b>e<sub>2</sub> (mm)</b>	83.15	83.15	0
<b>e<sub>3</sub> (mm)</b>	5	83.15	5
<b>a (mm)</b>	310	1125	615
<b>c (mm)</b>	310	1125	615
<b>α</b>	17.63		0.056721497
<b>A</b>	-16.63		0.943278503
<b>B</b>	0.137		1.89432785
<b>C</b>	0.9		0.9
<b>b/L</b>	0.2286		0.7714
<b>b (mm)</b>	708.5	5625.0	4744.4
<b>L-b (mm)</b>	2391.5	5625.0	1405.6
<b>θ<sub>B</sub> (rad)</b>	0.0141	0.0591	0.0372
<b>θ<sub>D</sub> (rad)</b>	0.0737	0.0591	0.0071
<b>θ (rad)</b>	0.1616	0.2365	0.0814
<b>μ(θ+kx)</b>	0.0373	0.0653	0.0261
<b>Pe<sup>-μ(θ+kx)</sup> (kN)</b>	815	764	744
<b>Draw in (mm)</b>	6		
<b>Loss per unit (kN/m)</b>	4.98		
<b>l (m)</b>	11.87		
<b>2pl (kN)</b>	118		
<b>Force at anchorage (kN)</b>	728		
<b>Span</b>	1-2	2-4	4-5
<b>Force per tendon (kN)</b>	771	789	754
<b>Force after long-term losses (kN)</b>	656	671	641
<b>Drape (mm)</b>	46.58	166.30	46.58
<b>P (kN)</b>	1052	3881	4142
<b>Tendons needed</b>	2	6	6

Table 4-4 Summary of determination of number of tendons for axis H

### 2.5.3. Results for the axis I

In Table 4-7, the results for the axis H are shown. The result indicates that the total loss is

$$\left(\frac{846-646}{846}\right)*100 \approx 25\%.$$

<b>Span</b>	6-4	4-3	3-2
<b>L (mm)</b>	15000	8750	3100
<b>e<sub>1</sub> (mm)</b>	0	83.15	83.15
<b>e<sub>2</sub> (mm)</b>	83.15	83.15	0
<b>e<sub>3</sub> (mm)</b>	83.15	0	5
<b>a (mm)</b>	1500	875	310
<b>c (mm)</b>	1500	875	310
<b>α</b>	2		0.056721497
<b>A</b>	-1		0.943278503
<b>B</b>	1.7		1.89432785
<b>C</b>	0.9		0.9
<b>b/L</b>	0.4238		0.7714
<b>b (mm)</b>	6356.6	4375.0	2391.5
<b>L-b (mm)</b>	8643.4	4375.0	708.5
<b>θ<sub>B</sub> (rad)</b>	0.0262	0.0380	0.0737
<b>θ<sub>D</sub> (rad)</b>	0.0385	0.0380	0.0141
<b>θ (rad)</b>	0.1031	0.1520	0.1616
<b>μ(θ+kx)</b>	0.0446	0.0444	0.0373
<b>Pe<sup>-μ(θ+kx)</sup> (kN)</b>	809	774	746
<b>Draw in (mm)</b>	6		
<b>Friction loss per unit (kN/m)</b>	3.74		
<b>l (m)</b>	13.70		
<b>Anchorage set loss (kN)</b>	102		
<b>Force at anchorage (kN)</b>	744		
<b>Span</b>	6-4	4-3	3-2
<b>Force per tendon (kN)</b>	776	792	760
<b>Force after long-term losses (kN)</b>	660	673	646
<b>Drape (mm)</b>	124.73	83.15	46.58
<b>P (kN)</b>	9200	4696	1052

Table 4-5 Summary of determination of number of tendons for axis I

It can be observed that the final pre-stressing loss is the studied axes is 25%. So from now on, in order to simplify the calculations, it will be assumed a loss of pre-stress including short-term and long-term effects of 25%.

#### 2.5.4. Results for axis 4

The results for axis 4 is the same for axis 9 and axis D because, as shown in the plan of the slab, these axis have the same spanning.

P after losses:  $0.75P_{\max} = 634.5 \text{ kN}$

Then with equation 4.1, the pre-stressing force needed and finally the number of tendons is determined.

Table 4-7 shows the number of tendons needed for every span of the axis 4. In the span E-G there will be no change of direction of the tendon because it is all under negative moment. Also in span I-K the number of tendons was reduced to 8 to have an even number of tendons with the adjacent spans.

Span	B-C	C-D	D-E	E-G	G-I	I-K	K-L	L-M
<b>L (mm)</b>	2500	8750	12945	4100	12950	15000	8750	2500
<b>e1</b>	0	83.15	83.15	83.15	83.15	83.15	83.15	83.15
<b>e2</b>	83.15	83.15	83.15	83.15	83.15	83.15	83.15	0
<b>e3</b>	5	0	83.15	-83.15	83.15	83.15	0	5
<b>Drape (mm)</b>	40.58	77.15	160.30	0.00	160.30	160.30	77.15	40.58
<b>P (kN)</b>	786	5061	5331	--	5336	7158	5061	786
<b>Tendons needed</b>	2	8	8	--	8	11	8	2
<b>Tendons provided</b>	2	8	8	2	8	8	8	2

Table 4-6 Summary of determination of number of tendons for axis 4

#### 2.5.5. Results for axis 6

Table 4-9 shows the number of tendons needed in axis 6 from A to H.

Span	A-B	B-D	D-F	F-H
<b>L (mm)</b>	4000	15000	11250	3750
<b>e1</b>	0	83.15	83.15	0
<b>e2</b>	83.15	83.15	83.15	83.15
<b>e3</b>	10	83.15	10	5
<b>Drape (mm)</b>	51.58	160.30	93.15	46.58
<b>P (kN)</b>	1582	7158	6929	1540
<b>Tendons needed</b>	2	11	11	2

Table 4-7 Summary of determination of number of tendons for axis 6

### 2.5.6. Results for axis 7

Table 4-10 shows the number of tendons needed in axis 7 from D to H.

Span	D-F	F-H
<b>L (mm)</b>	15000	6000
<b>e1</b>	0	83.15
<b>e2</b>	83.15	0
<b>e3</b>	83.15	41.575
<b>Drape (mm)</b>	124.73	41.58
<b>P (kN)</b>	9200	4416
<b>Tendons needed</b>	14	7

Table 4-8 Summary of determination of number of tendons for axis 7

## 2.6. Modeling of the pre-stressing

The modeling of the pre-stressing was done in the software SCIA as well. This software has three possibilities of modeling for this:

- Definition of the equivalent load: modeling the equivalent effects of the tendon in the slab
- Real tendon in a 1D rib: The tendon is defined in a fictive 1D rib which is part of the 2D slab
- Real tendon in the 2D member directly: The tendon is defined directly in the 2D member using a “hanging node” [22]



Due to the experience of modeling the slab in this software explained in section 4.3, it was decided to use the equivalent method to model the pre-stressing. This method takes more time, but it simplifies the inputs so that we do not have to depend of the features of the program to retrieve proper results and the calculation of this inputs helps the author to understand more in depth the effects of the pre-stressing in the structure.

### 2.6.1. Calculation of equivalent loads

The calculation of the equivalent loads of axis F from 4-9 will be shown as an example.

#### 5.6.1.1. Results for axis F

Taking figure 4-6 as a reference,  $L_3$  will be assumed as

$$L_3 = c_{col} + d_h$$

In which  $c_{col}$  is the diameter of the column (900mm) and  $d_h$  is the distance of the center of the strand and the lower surface of the slab.

$$d_h = d - c_d + 2 * \phi + 0.5 * 15.7 = 300 - 66.85 = 233.15 \text{ mm}$$

$$L_3 = 900 + 233.15 = 1133.15 \text{ mm}$$

Then we calculate the horizontal component H of the pre-stressing force  $P_{prov}$  and  $\beta$  is the angle of the prestressing force in the beginning of every span. Then we calculate the force per meter h for the length of our column strip.

$$\beta = \frac{e_1 + e_3}{0.4 L} = \frac{0 + 83.15}{0.4 \times 15000} = 0.01$$

$$H = P_{prov} \cos(\beta) = 14 * 634.5 * \cos(0.01) = 8882 \text{ kN}$$

$$h = 8882 / 6 = 1480 \text{ kN/m}$$

$$L_1 = l_1 - L_2 / 2 = 15000 - 1133 / 2 = 14433.5 \text{ mm}$$

And then  $p_1$  is calculated with equation 4.1 and we will divide it by the length of the column strip.

$$p_1 = \frac{8 \times 0.124 \times 8882}{14.433 \times 6} = 7.10 \text{ kN/m}^2$$

From Figure 4-6, is assumed a vertical length of  $f_v = 12 \text{ mm}$  between the center of the strand and the inflection point. This is the drape used to calculate the force  $V$  per length of column strip.

$$V = \frac{8 \times 0.012 \times 8882}{1133 \times 6} = 110.71 \text{ kN/m}^2$$

Table 4-11 shows the calculation for the rest of spans.

Span	4-6	6-7	7-9
<b>L3 (mm)</b>	1133	1133	1133
<b>0.4L (mm)</b>	6000	6000	6000
<b><math>\beta</math> (rad)</b>	0.01	0.02	0.03
<b>H (kN)</b>	8882	8881	8880
<b>h(kN/m)</b>	1480	1480	1480
<b>L (mm)</b>	14434	14434	14434
<b>p (kN/m<sup>2</sup>)</b>	7	7	7
<b>f(mm)</b>	12	12	12
<b>V (kN/m<sup>2</sup>)</b>	111	111	111

Table 4-9 Calculation of equivalent forces for pre-stressing in axis F

Values  $h$  as a line force, and  $p$  and  $V$  as surface loads are introduced in the software in every column strip.

### 5.6.1.2. Results for axis I

Table 4-12 shows the equivalent loads for the pre-stressing in axis I from 1-5. In the span 1-2 is required only 2 tendons and in 2-4 and 4-5, 6 tendons. So in 2, 4 more tendons will be introduced and anchored in 5. To represent the effect of the 4 extra tendons, an additional force of  $(H_{2-4} - H_{1-2})/6 = 422.6 \text{ kN/m}^2$  is added in 2. In the same way the additional forces are calculated for the rest of the axes.

Span	1-2	2-4	4-5
<b>L3 (mm)</b>	1133	1133	1133
<b>0.4L (mm)</b>	1240	4500	2460
<b><math>\beta</math> (rad)</b>	0.00	0.04	0.04
<b>H (kN)</b>	1269	3804	3805
<b>h(kN/m)</b>	211	634	634
<b>L (mm)</b>	2534	10684	5584
<b>p (kN/m<sup>2</sup>)</b>	12	7	8
<b>f(mm)</b>	12	12	12
<b>V (kN/m<sup>2</sup>)</b>	16	47	47
<b>Additional force (kN/m)</b>		423	

Table 4-10 Calculation of equivalent forces for pre-stressing in axis I

### 5.6.1.3. Results for axis K

Table 4-13 shows the equivalent loads for the pre-stressing in axis K from 6-2.

Span	6-4	4-3	3-2
<b>L3 (mm)</b>	1133	1133	1133
<b>0.4L (mm)</b>	6000	3500	1240
<b><math>\beta</math> (rad)</b>	0.01	0.02	0.07
<b>H (kN)</b>	8882	4440	1266
<b>h(kN/m)</b>	1480	740	211
<b>L (mm)</b>	14434	8184	2534
<b>p (kN/m<sup>2</sup>)</b>	7	7	12
<b>f(mm)</b>	12	12	12
<b>V (kN/m<sup>2</sup>)</b>	111	55	16
<b>Additional force (kN/m)</b>		740	529

Table 4-11 Calculation of equivalent forces for pre-stressing in axis K

### 5.6.1.4. Results for axis 4

Table 4-14 shows the equivalent loads for the pre-stressing in axis 4 from B-M.

Span	B-C	C-D	D-E	E-G	G-I	I-K	K-L	L-M
<b>L3 (mm)</b>	1141	1141	1141		1141	1141	1141	1141
<b>0.4L (mm)</b>	1000	3500	5178		5180	6000	3500	1000
<b><math>\beta</math> (rad)</b>	0.01	0.02	0.03		0.03	0.03	0.02	0.09
<b>H (kN)</b>	1269	5075	5073		5073	5074	5075	1264
<b>h(kN/m)</b>	211	846	846		846	846	846	211
<b>L (mm)</b>	1930	7609	11804		11809	13859	7609	1930
<b>p (kN/m<sup>2</sup>)</b>	18	9	8		8	6	9	18
<b>f(mm)</b>	12	12	12		12	12	12	12
<b>V (kN/m<sup>2</sup>)</b>	16	62	62		62	62	62	16
<b>Additional force (kN/m)</b>		634			634			

Table 4-12 Calculation of equivalent forces for pre-stressing in axis 4

### 5.6.1.5. Results for axis 6

Table # shows the equivalent loads for the pre-stressing in axis 6 from A-H.

Span	A-B	B-D	D-F	F-H
<b>L3 (mm)</b>	1141	1141	1141	1141
<b>0.4L (mm)</b>	1600	6000	4500	1500
<b><math>\beta</math> (rad)</b>	0.01	0.03	0.02	0.00
<b>H (kN)</b>	1269	6977	6978	1269
<b>h(kN/m)</b>	211	1163	1163	211
<b>L (mm)</b>	3430	13859	10109	3180
<b>p (kN/m<sup>2</sup>)</b>	7	8	8	8
<b>f(mm)</b>	12	12	12	12
<b>V (kN/m<sup>2</sup>)</b>	16	86	86	16
<b>Additional force (kN/m)</b>		951		

Table 4-13 Calculation of equivalent forces for pre-stressing in axis 6

### 5.6.1.6. Results for axis 7

Table 4-16 shows the equivalent loads for the pre-stressing in axis 6 from D-H.

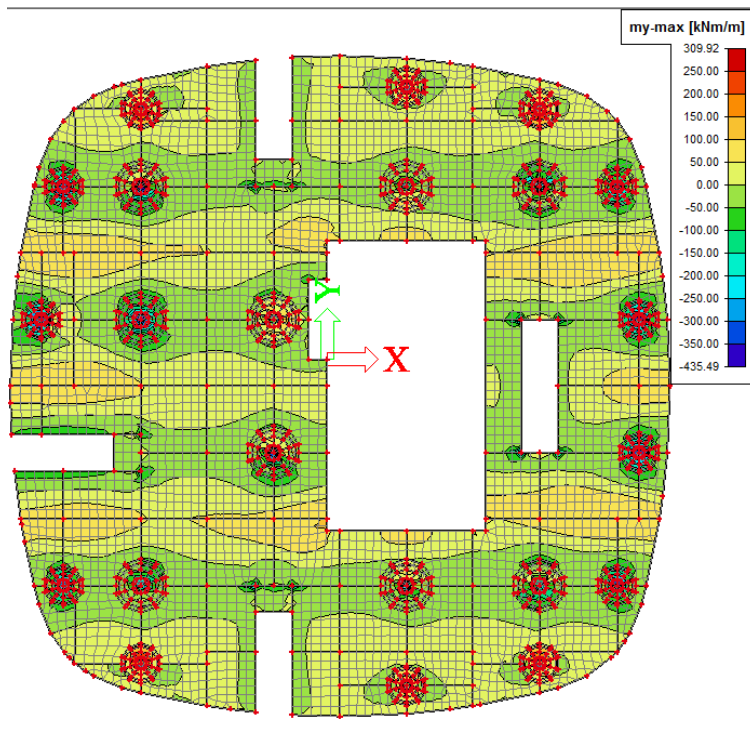
Span	D-F	F-H
<b>L3 (mm)</b>	1141	1141
<b>0.4L (mm)</b>	6000	2400
<b><math>\beta</math> (rad)</b>	0.01	0.05
<b>H (kN)</b>	9517	4436
<b>h(kN/m)</b>	1586	739
<b>L (mm)</b>	14430	4859
<b>p (kN/m<sup>2</sup>)</b>	8	10
<b>f(mm)</b>	12	12
<b>V (kN/m<sup>2</sup>)</b>	117	55
<b>Additional force (kN/m)</b>	847	

Table 4-14 Calculation of equivalent forces for pre-stressing in axis 7

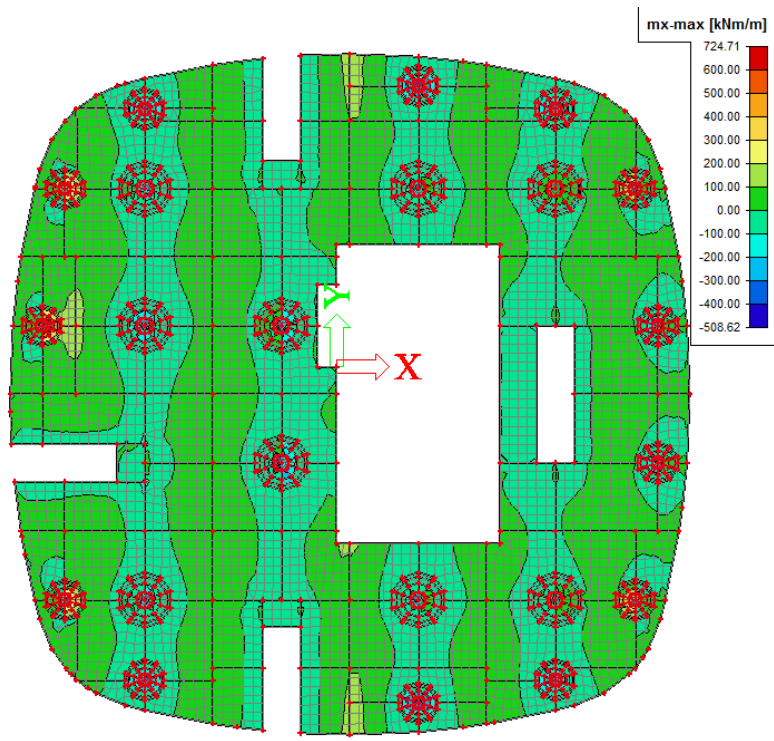
## 2.7. Analysis in SCIA

### 2.7.1. Analysis for dead load + load pattern 1 + pre-stress

Figure 4-13 a-c shows the diagram of moment x, moment y and deformation for dead load + load pattern 1 + pre-stress in SLS.



(a) My



(b) Mx

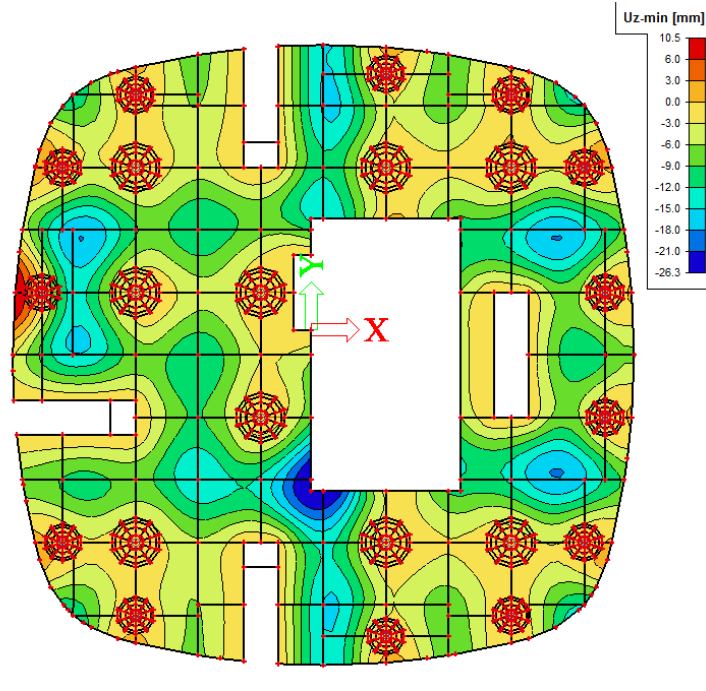
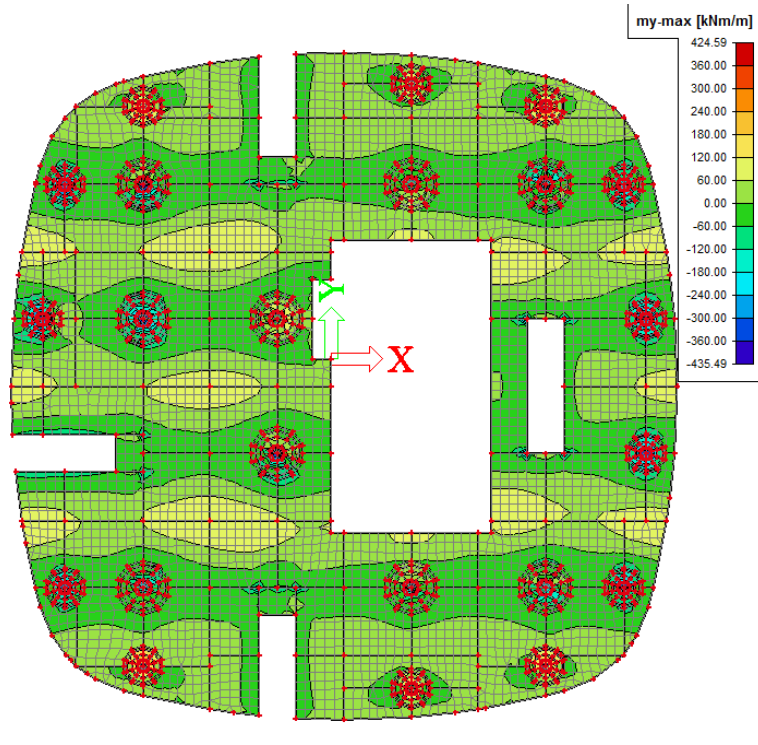


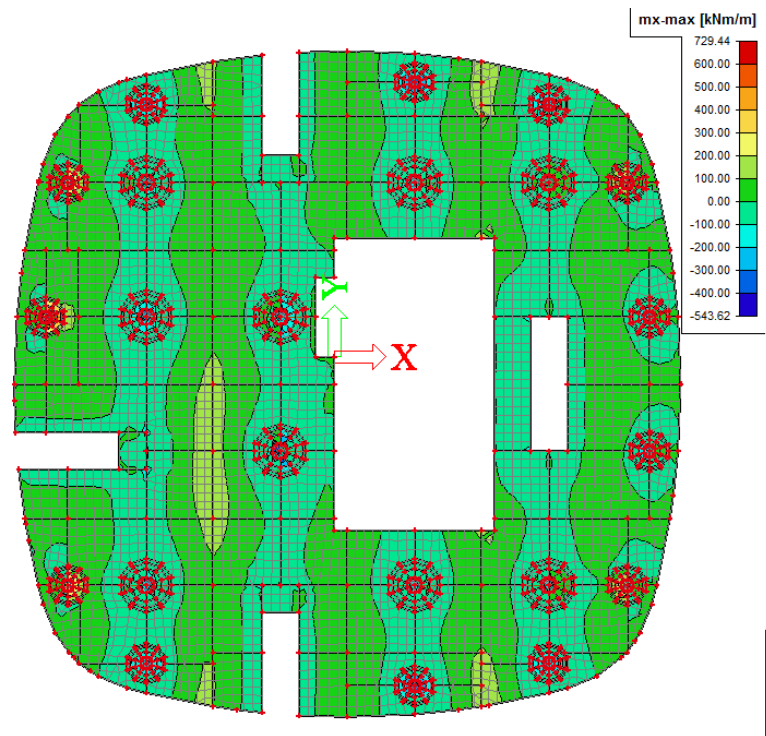
Figure 4-13 Diagram for dead load + load pattern 1 + pre-stress

### 2.7.2. Analysis for dead load + load pattern 2 + pre-stress

Figure 4-14 a-c shows the diagram of moment x, moment y and deformation for dead load + load pattern 2 + pre-stress in SLS.



(a) My



(b) Mx



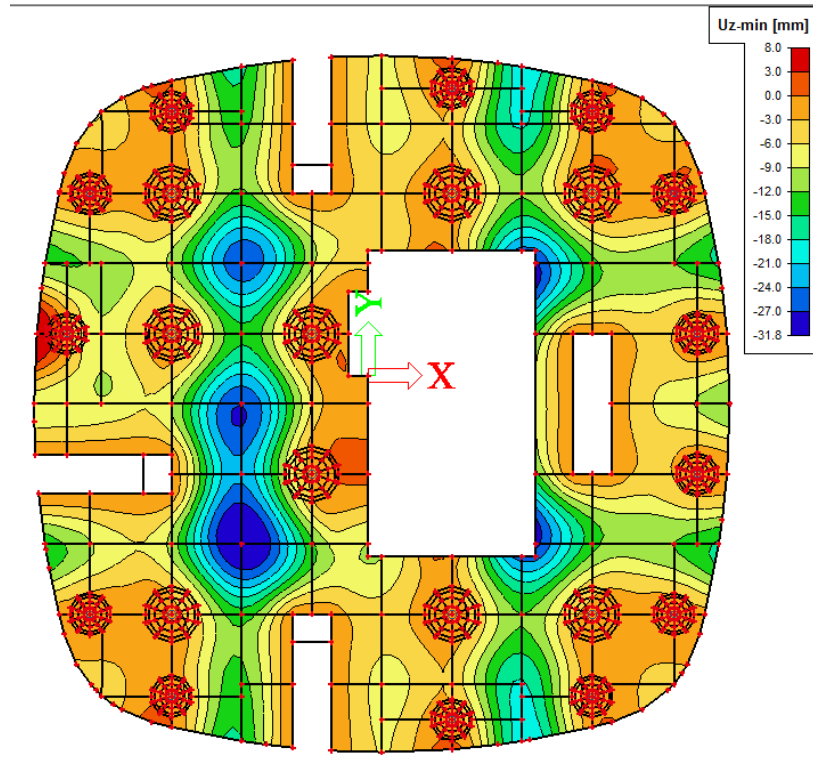
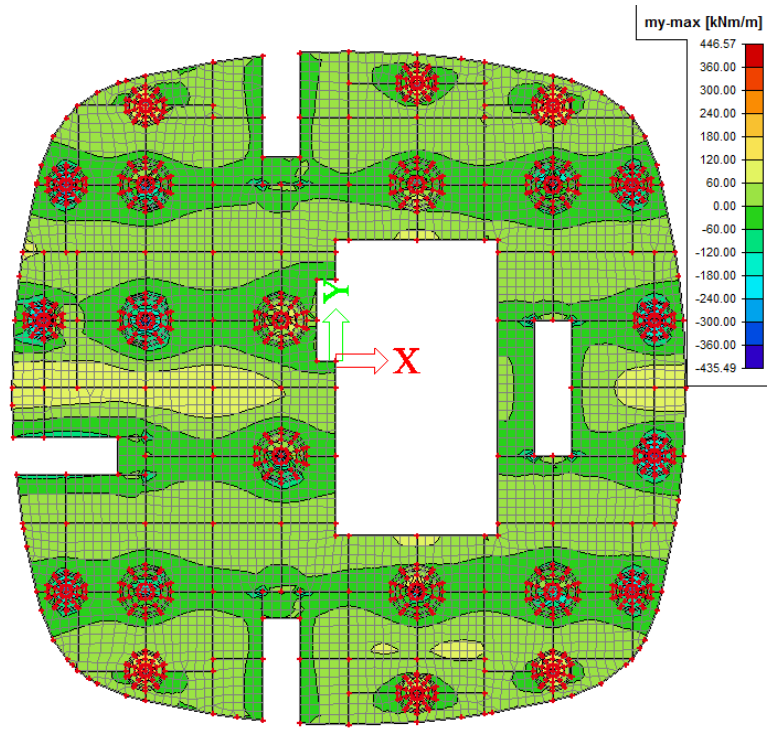


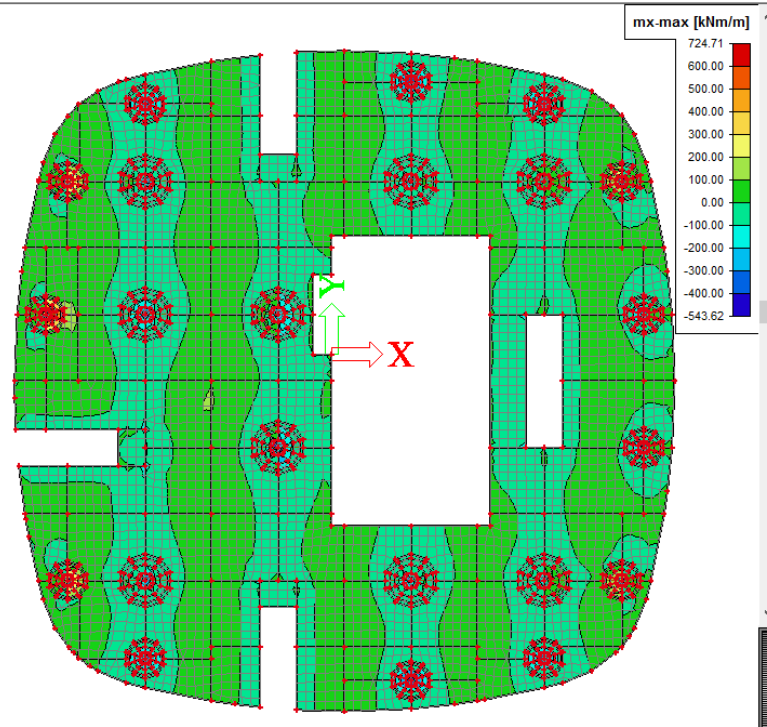
Figure 4-14 Diagram for dead load + load pattern 2 + pre-stress

### 2.7.3. Analysis for dead load + load pattern 3 + pre-stress

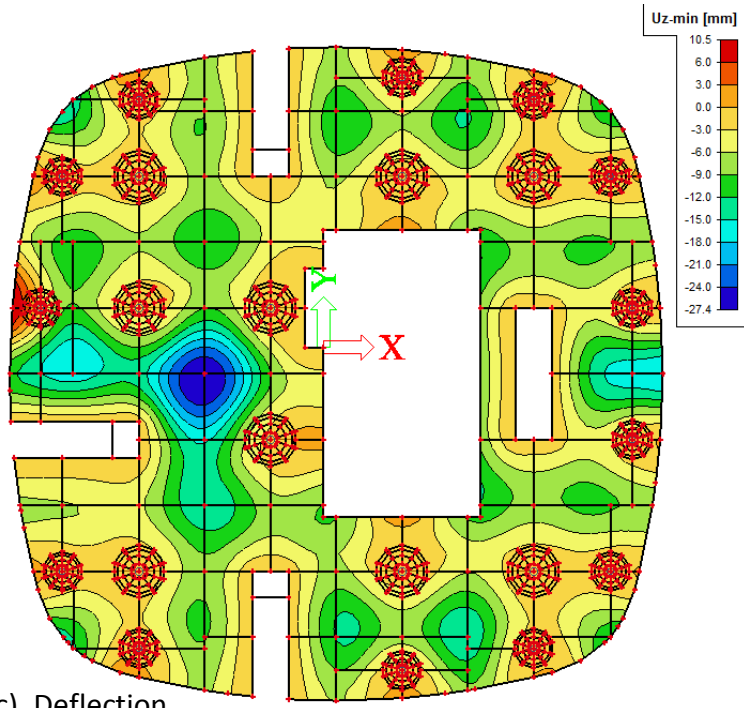
Figure 4-15a-c shows the diagram of moment x, moment y and deformation for dead load + load pattern 3 + pre-stress in SLS.



(a) My



(b) Mx

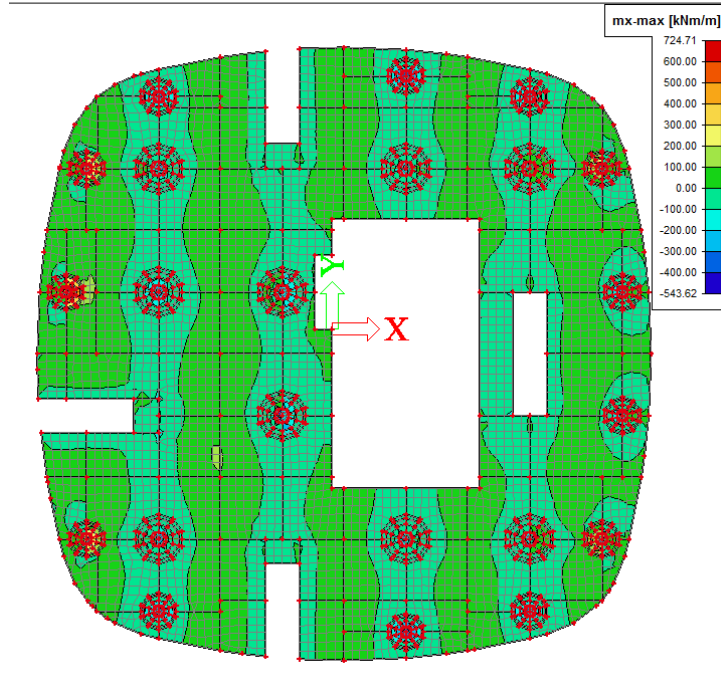


(c) Deflection

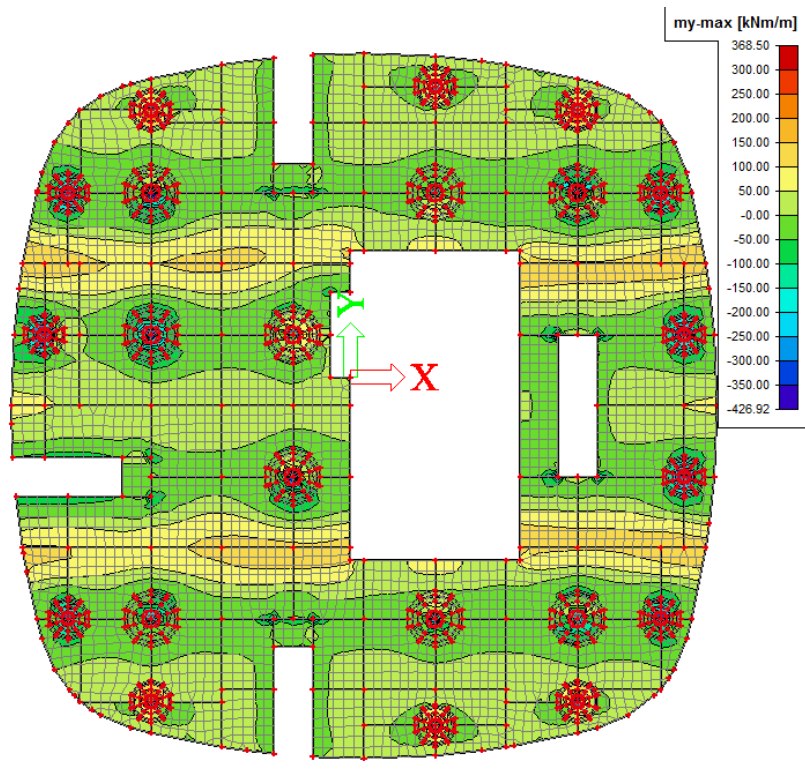
Figure 4-15 Diagram for dead load + load pattern 3 + pre-stress

#### 2.7.4. Analysis for dead load + load pattern 4 + pre-stress

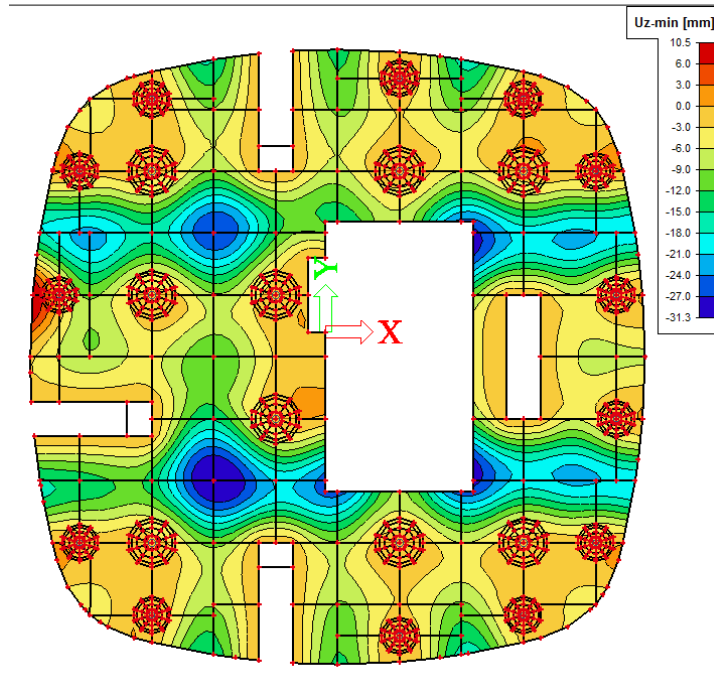
Figure 4-16a-c shows the diagram of moment x, moment y and deformation for dead load + load pattern 4 + pre-stress in SLS.



(a) My



(b) Mx

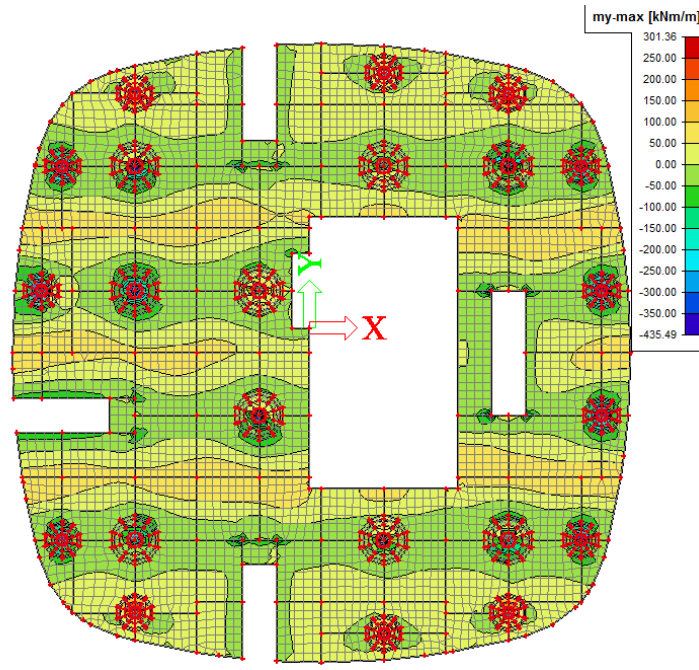


(c) Deflection

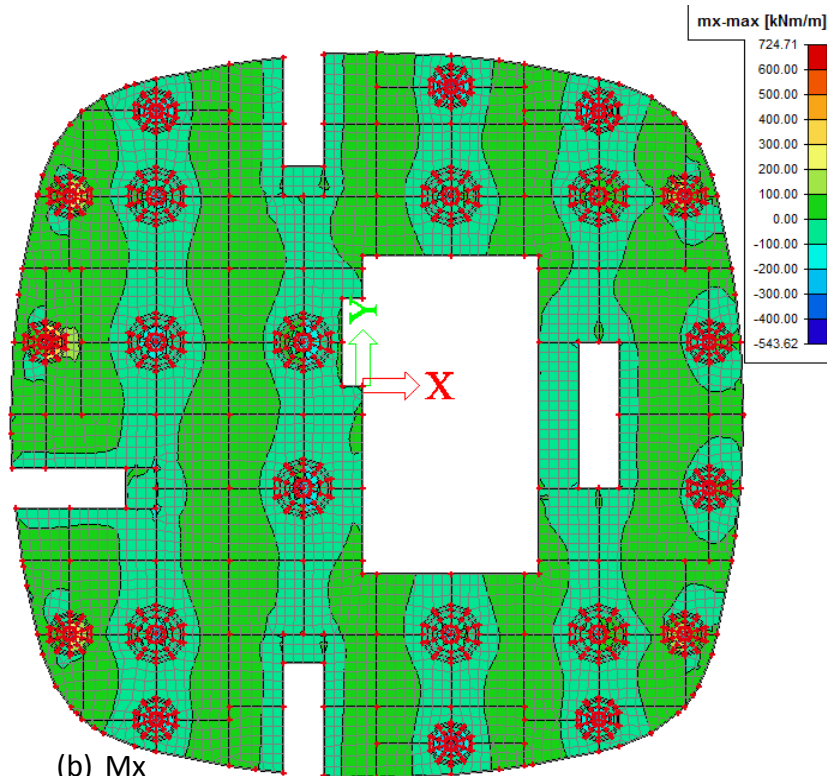
Figure 4-16 Diagram for dead load + load pattern 4 + pre-stress

### 2.7.5. Analysis for dead load + load pattern 5 + pre-stress

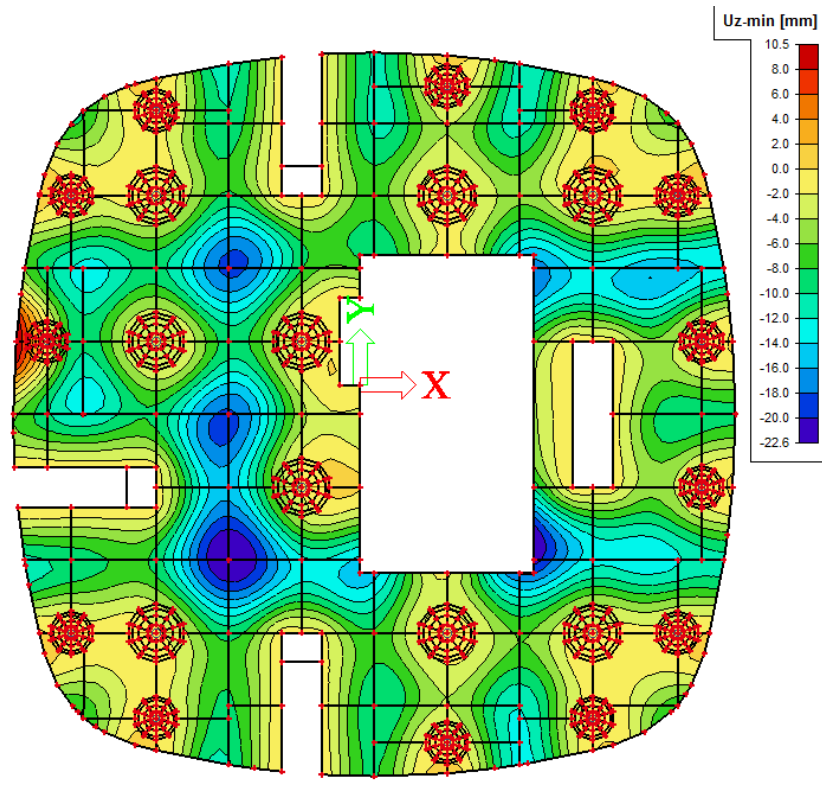
Figure 4-17 a-c shows the diagram of moment x, moment y and deformation for dead load + load pattern 5 + pre-stress in SLS.



(a)  $M_y$



(b)  $M_x$



(c) Deflection

Figure 4-17 Diagram for dead load + load pattern 5 + pre-stress

## 2.8. Assessment of results and check

In contrast with the output of the analysis performed in section 4.3, it can be observed that the negative moments have diminished in large quantity. It still can be found some peak positive moments and negative moments in the supports. This can be solved by increasing the size of the averaging strips in the supports. In the other hand, Table 4-17 Comparison of deflection with and without pre-stress shows that the maximum deflection has been reduced 30 %.

Load pattern	Deflection conventional concrete (mm)	Deflection pre-stressed concrete (mm)	Reduction (%)
Load pattern 1	36.5	26.3	28
Load pattern 2	40.9	31.8	22
Load pattern 3	34.9	27.4	21
Load pattern 4	40.4	31.3	23
Load pattern 5	32.3	22.6	30

Table 4-15 Comparison of deflection with and without pre-stress

We will check the results by performing the SLS and ULS check. The reinforcement will be design and checked only for the area delimited by axes 6, 7, D and F. The points A, B, C, D, E, F, G, H, I were determined (Figure 4-18 Area delimited by axis 6,7,D and F).

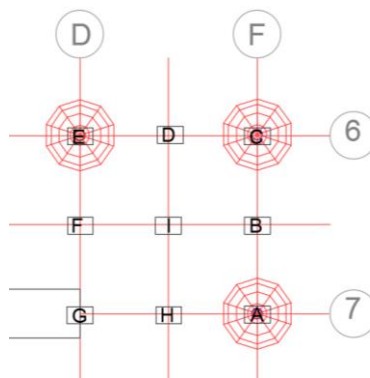


Figure 4-18 Area delimited by axis 6,7,D and F

### 2.8.1. ULS check

For example for point B we took the values for the moment in the axis x ( $B_x$ ) and the axial force shown in table # from SCIA. It was checked for a one-meter-width strip.

$b = 1 \text{ m}$

Load Patterns	By
Load pattern 1	34.00
Load pattern 2	57.80
Load pattern 3	79.90
Load pattern 4	22.10
Load pattern 5	46.75

Table 4-16 Moment in y axis on point B



$$d_1 = c_d + 1.5\phi = 0.04 \text{ m}$$

$$d^* = d - c_d - 1.5\phi = 0.26 \text{ m}$$

Equation 4.11 give us the depth of concrete in compression after cracking in order to calculate the force in the concrete and the required area of steel.

$$x_b = d^* - \sqrt{d^{*2} - \frac{M_{Ed} - N_{Ed}(0.5d - d_1)}{0.5bf_{cd}}} \quad (4.11)$$

$$x_b = 0.26 - \sqrt{0.26^2 - \frac{0.079 + 0.196 \times (0.5 \times 0.30 - 0.04)}{0.5 \times 23.33}} = 0.0174 \text{ m}$$

$$F_{cd} = x_b f_{cd} = 0.41 \text{ MN}$$

$$A_{s,rqd} = \frac{(F_d + N)}{f_{yd}} = 483 \text{ mm}^2$$

Now the minimum and maximum area of steel is calculated with the following conditions.

$$A_{s,max} = 0.04 bd = 12000 \text{ mm}^2$$

$$A_{s,min} = 0.0015 bd = 361.5 \text{ mm}^2$$

$$A_{s,min} = 0.26 f_{ctm} d^* / f_{yk} = 401 \text{ mm}^2$$

$$A_{s,min\sigma s} = \frac{k_c k f_{ct,eff} A_{ct}}{\sigma_s} \quad (4.12)$$

In which  $k_c$  depends of the stress distribution and  $k$  represents the effect of the non-uniform self-equilibrating effects. In this case, for bending it will be assumed a value of  $k_c = 0.4$  and  $k=1$ .

$A_{ct}$  is the area of concrete in tension.

$$A_{s,min\sigma s} = \frac{1 \times 0.4 \times 2.2 \times (1000 * 300 * 0.5)}{435} = 303 \text{ mm}^2$$

In conclusion, the  $A_{s,min}$  is

$$A_{smin} = \max(361.5; 401; 303) = 401 \text{ mm}^2$$

The chosen reinforcement is  $\phi 12\text{mm}$  every 150 mm.

$$A_{prov} = 565.5 \text{ mm}^2$$

With this, the force in the steel and in the concrete will be calculated and therefore the resistant moment.

$$F_{s,d} = A_{prov} f_{yd} = 0.25 \text{ MN}$$

$$x_b = (F_{s,d} - N) / f_{cd} = 0.019 \text{ m}$$

$$x_{b,lim} = 0.127 \text{ m} > x_b$$

$$F_{cd} = x_b f_{cd} b = 0.44 \text{ MN}$$

$$M_{Rd} = F_{cd} (0.5d - 0.5x_b) + F_{sd} (d^* - 0.5d) = 1.57 \text{ MN} > M_{Ed}$$

The same was done for the aforementioned points. Table # shows the results.

## 2.8.2. SLS check

Exposure Class	Reinforced members and prestressed members with unbonded tendons	Prestressed members with bonded tendons
	Quasi-permanent load combination	Frequent load combination
X0, XC1	0,4 <sup>1</sup>	0,2
XC2, XC3, XC4	0,3	0,2 <sup>2</sup>
<sup>AC2</sup> XD1, XD2, XD3, XS1, XS2, XS3 <sub>AC2</sub>		Decompression
<p><b>Note 1:</b> For X0, XC1 exposure classes, crack width has no influence on durability and <sup>AC1</sup>this limit is set to give generally acceptable appearance. In the absence <sub>AC1</sub> of appearance conditions this limit may be relaxed.</p> <p><b>Note 2:</b> For these exposure classes, in addition, decompression should be checked under the quasi-permanent combination of loads.</p>		

Table 4-17 Conditions for SLS check

The structure is pre-stressed with unbonded tendons and has exposure class XC1. Therefore, to perform this check, according to Table 4-19 Conditions for SLS checkTable 4-19, it is enough to calculate the crack width with a quasi permanent load combination which in this case, the maximum must be  $w_{max} = 0.4$  mm. It was checked for the points F, I and B in the y direction.

This was calculated with the equations 4.13, 4.14 and 4.15.

$$w_k = s_{r,max}(\varepsilon_{sm} - \varepsilon_{cm}) \quad (4.13)$$

$$\varepsilon_{sm} - \varepsilon_{cm} = \frac{\sigma_s - k_t \frac{f_{ct,eff}}{\rho_{p,eff}} (1 + \alpha_e \rho_{p,eff})}{E_s} \geq 0.6 \frac{\sigma_s}{E_s} \quad (4.14)$$

$$s_{r,max} = k_3 c + k_1 k_2 k_4 \phi / \rho_{p,eff} \quad (4.15)$$

In which

- $s_{r,max}$  is the maximum crack spacing.
- $\epsilon_{sm}$  is the mean strain in the reinforcement under the relevant combination of loads, including the effect of imposed deformations and taking into account the effects of tension stiffening. Only the additional tensile strain beyond the state of zero strain of the concrete at the same level is considered.
- $\epsilon_{cm}$  is the mean strain in the concrete between cracks
- $\sigma_s$  is the stress in the tension reinforcement assuming a cracked section.
- $\alpha_e$  is the ratio  $E_s/E_{cm}$
- $\rho_{p,eff} = (A_s)/A_{c,eff}$
- $k_t$  is a factor dependent on the duration of the load ( $k_t = 0,4$  for long term loading)
- $c$  is the cover to the longitudinal reinforcement
- $k_1$  is a coefficient which takes account of the bond properties of the bonded reinforcement: ( $k_1 = 0.8$  for high bond bar)
- $k_2$  is a coefficient which takes account of the distribution of strain: ( $k_2 = 0,5$  for bending)
- The recommended values for  $k_3$  and  $k_4$  are 3.4 and 0.425 respectively

$\sigma_s$  was taken from SCIA.  $A_{c,eff}$  is calculated like in Figure 4-19 in where B is  $A_{c,eff}$ .

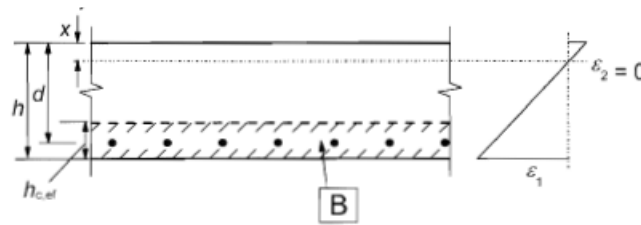


Figure 4-19 Calculation of  $A_{c,eff}$  in slab

	Fy	Iy	By
<b><math>\sigma_s</math> (Mpa)</b>	9.7	6.8	5.2
<b>As (mm<sup>2</sup>)</b>	565.49	3141.59	753.98
<b><math>\phi</math> (mm)</b>	12	20	12
<b>Aceff (mm)</b>	82000	90000	82000
<b><math>\rho_p, \text{eff}</math></b>	0.006896	0.034907	0.009195
<b><math>\epsilon_{sm} - \epsilon_{cm}</math></b>	4.52E-05	3.033E-05	2.2E-05
<b><math>\epsilon_{sm} - \epsilon_{cm} \text{ lim}</math></b>	2.98E-05	2.092E-05	1.6E-05
<b>sr,max (mm)</b>	414.8	216.4	340.9
<b>wk (mm)</b>	0.01876	0.00656	0.00755

Table 4-18 Calculation of maximum crack width

Load Patterns	Ax	Av	Bx	By	Cx	Cy	Dx	Dy	Ex	Ey	Fx	Fy	Gx	Gy	Hx	Hy	Ix	Iy	
Load pattern 1	-404.95	-365.16	-30.00	34.00	-139.50	-471.66	34.85	-52.00	-351.65	-487.00	-487.00	-39.00	65.45	-169.00	-250.75	53.55	-42.00	64.00	56.00
Load pattern 2	-273.00	-409.50	-59.00	57.80	-448.50	-448.50	113.90	-81.00	-583.05	-469.30	-469.30	-78.00	84.00	-213.00	-482.00	169.00	-41.00	179.00	112.00
Load pattern 3	-383.50	-321.75	-38.00	79.90	-509.25	-577.15	71.40	-68.00	-513.50	-594.75	-594.75	-62.00	138.00	-123.00	-499.00	115.00	-47.00	143.00	132.00
Load pattern 4	-370.50	-484.90	-48.00	22.10	-202.50	-229.50	76.50	-66.00	-422.50	-399.10	-399.10	-49.00	43.00	-198.00	-220.00	63.00	-50.00	63.00	55.00
Load pattern 5	-434.20	-468.00	-44.00	46.75	-357.75	-405.45	74.80	-68.00	-427.05	-570.60	-570.60	-57.00	82.00	-87.00	-388.00	114.00	-49.00	106.00	88.00
<b>Envelope</b>																			
N	-800.00	-911.00	-196.00	-196.00	-810.00	-922.00	-690.00	-525.00	-600.00	-710.00	-710.00	280.00	-913.00	-1170.00	-600.00	-575.00	540.00	179.00	132.00
b(m)	1.00	1.00	1.00	1.00	1.00	1.00	1.00	1.00	1.00	1.00	1.00	1.00	1.00	1.00	1.00	1.00	1.00	1.00	1.00
d1(m)	0.06	0.04	0.06	0.04	0.06	0.04	0.06	0.04	0.06	0.04	0.06	0.06	0.04	0.06	0.04	0.06	0.04	0.06	0.04
d(m)	0.24	0.26	0.24	0.24	0.24	0.26	0.24	0.26	0.24	0.26	0.24	0.24	0.26	0.24	0.26	0.24	0.26	0.24	0.26
xb (mm)	0.1200965	0.1300203	0.0140768	0.0174137	0.1509674	0.1669186	0.0337948	0.0239990	0.1825408	0.1645311	0.0095294	0.0428531	0.0658031	0.1237040	0.0432436	-0.0012943	0.0256058	0.0100035	0.0100035
Fcd (MN)	2.80	3.03	0.33	0.41	3.52	3.89	0.79	0.56	4.26	3.84	3.84	0.22	1.00	1.54	2.89	1.01	-0.03	0.60	0.23
Asrpd (mm2)	4601.96	4879.02	304.40	483.36	6234.64	6832.67	226.28	80.22	8410.75	7191.98	7191.98	1154.76	199.45	839.51	5255.21	997.41	1171.96	2451.45	2108.93
smin	37.00	37.00	37.00	37.00	37.00	37.00	37.00	37.00	37.00	37.00	37.00	37.00	37.00	37.00	37.00	37.00	37.00	37.00	37.00
Asrpd (mm2)	4188.79	4188.79	565.49	4188.79	4188.79	4188.79	565.49	565.49	4188.79	4188.79	4188.79	1340.41	565.49	1130.97	4188.79	1130.97	1340.41	2680.83	3141.59
Asrpd	@	@	@	@	@	@	@	@	@	@	@	@	@	@	@	@	@	@	@
Asrpd>Asrpd	NO!	NO!	OK	OK	NO!	NO!	OK	OK	NO!	NO!	OK	OK	OK	NO!	OK	OK	OK	OK	OK
Fsd (MN)	1.82	1.82	0.25	0.25	1.82	1.82	0.25	0.25	1.82	1.82	1.82	0.58	0.25	0.49	1.82	0.49	0.58	1.17	1.37
xb (m)	0.11239279	0.11715061	0.01894499	0.01894499	0.11282142	0.11762211	0.04011945	0.03304701	0.10382013	0.10853509	0.01299098	0.04967796	0.07123761	0.10382013	0.04573397	0.00184653	0.02988252	0.02925816	0.02925816
xb (mm)	0.11890749	0.12680176	0.11890749	0.12680176	0.11890749	0.12680176	0.11890749	0.12680176	0.11890749	0.12680176	0.11890749	0.12778855	0.11890749	0.12680176	0.11890749	0.12680176	0.11890749	0.12680176	0.12680176
xb>xb,lim	OK	OK	OK	OK	OK	OK	OK	OK	OK	OK	OK	OK	OK	OK	OK	OK	OK	OK	OK
Fcd (MN)	2.62	2.73	0.44	0.44	2.63	2.74	0.94	0.77	2.42	2.53	2.53	0.30	1.16	1.66	2.42	1.07	0.04	0.70	0.68
Md (MNm)	0.74	0.71	1.57	1.57	0.74	0.71	1.32	1.41	0.84	0.82	0.82	1.70	1.22	1.00	0.87	1.30	1.83	1.59	1.66
Md>Med	OK	OK	OK	OK	OK	OK	OK	OK	OK	OK	OK	OK	OK	OK	OK	OK	OK	OK	OK

Table 4-19 ULS check of part of the slab

## 5. Conclusions

---

Pre-stressed concrete, as seen throughout this thesis, is a very useful technology. The first analysis showed the limitations of conventional concrete to be used in structure in which is desirable large spans. However, for the constructive process of such technology is necessary well-trained workforce, supervision and detailing in every step of this process in order to achieve the results for what it was design. Moreover, the quality of the materials used have to be superb to avoid pre-stressing losses and an adequate structural performance during service life.

The detailed calculation of the short term losses gave us the same range of loss for the three spans examined. Thus it can be concluded that the calculation for the pre-stressing losses can be accurately estimated with a range of 25%. Nonetheless, is recommended to perform this analysis when the span is short due to the fact that friction losses are increased the shorter the span.

The results for the ULS check was satisfactory for the majority of the sections. Nevertheless, the results for the column sections A, C and E showed that it does not have enough moment capacity, although the solutions for the steel area proposed are very similar. This can occur because of peak negative moments in the software and could be avoid by the addition of average strip of bigger area. In the case of the calculation of the moment being accurate, then other way to mitigate the lack of resistant moment would be by enhancing the pre-stressing force ensuring that stress limits are not violated.

Due to the complexity of the structure, a thorough design and check was not possible for this thesis and many assumptions were made to simplify the calculations. Yet the results for the deflections and the SLS check were satisfactory and it validates the solution presented.

The experience with the software SCIA engineer was very interesting. In the case of the modeling of the structure, due to the complexity of the slab, the availability of time and the inexperience of the author there was no option than using the software. But the modeling required a lot of time. In the case of the modeling of the pre-stressing, the time spent in

calculating the effects of the pre-stressing was considerable too. Calculation using a FEM software can be very sometimes is preferred because of the simplicity and the rapidity of the calculation. However, can be concluded that is always better, as far as possible, to use hand calculation instead of a FEM software.

## References

---

- [1] Gerwick Jr, B. C. (1997). *Construction of prestressed concrete structures*. John Wiley & Sons.
- [2] Hewson, N. R. (2003). *Prestressed concrete bridges: design and construction*. Thomas Telford.
- [3] Quintanilla Huayta, D. (2017). Ensayos experimentales en vigas de concreto postensado con tendones adheridos y no adheridos.
- [4] Raju, N. K. (2006). *Prestressed concrete*. Tata McGraw-Hill Education.
- [5] Kábelová A. (2010). *The national technical library – A new dominant feature of Prague*. Prague, Czech Republic: [www.czech.cz](http://www.czech.cz)
- [6] Krueger, S (2016) *The Building*. National Technical Library web page. Prague, Czech Republic: <https://www.techlib.cz/en/2755-the-building>
- [7] Abdel-Ghaffar, M. (2014). “Prestressed concrete”. Accessed 02 Apr 2017: <https://www.accessscience.com/content/prestressed-concrete/544100>



- [8]Nawy, E. G. (2011). *Prestressed concrete*. Pearson Education.
- [9]Bhatt, P. (2012). *Prestressed concrete design to Eurocodes*. CRC Press.
- [10]Sokal, P. DESIGN OF TWO-WAY PRESTRESSED SLABS.
- [11]Walraven, J.C. (2016). *Course CIE 3150 / CIE 4160 Prestressed concrete*.
- [12]ArchDaily (2009) "National Technical Library in Prague / Projektil Architekti" 31 Jul 2009. Accessed 30 Mar 2017. Recuperado de: <http://www.archdaily.com/29600/national-technical-library-in-prague-projektil-architekti/>
- [13]Naaman, A. E. (1982). *Prestressed concrete analysis and design: fundamentals* (pp. 360-364). New York: McGraw-Hill.
- [14]Nilson Arthur, H., David, D., & Dolan Charles, W. (2004). *Design of Concrete Structure*. The McGraw-Hill Company.
- [15]Procházka, J., & Štemberk, P. (2009). *Design Procedures for Reinforced Concrete Structures*. České vysoké učení technické.
- [16]British Standards Institution. (2004). *Eurocode 1: Actions on Structures. Part 1-1. General Actions; Densities, Self-weight, Imposed Loads for Buildings*. BSI.
- [17]British Standards Institution. (2004). *Eurocode 2: Design of Concrete Structures: Part 1-1: General Rules and Rules for Buildings*. British Standards Institution.
- [18]SCIA (2014, February 20). [EN] Handling result peaks on surfaces with Scia Engineer. Recuperado de: <https://www.youtube.com/watch?v=xAqEH7JVEvA>
- [19]NAVRÁTIL, J. (2014). *Prestressed concrete structures*. Ostrava: Technical University of Ostrava, Faculty of Civil Engineering, 2014, 220 s. ISBN 978-80-248-3625-6.
- [20]Wan, T. (1989). European Technical Approval ETA-13/0795. *Official Journal of the European Communities n L*, 40, 12.
- [21]SCIA (2015) *Advanced Expert Training Post-tensioning*. SCIA Engineer.

[22]SCIA (2015) *Post-tensioned concrete slab EN1992-1-1*. SCIA Engineer Help.

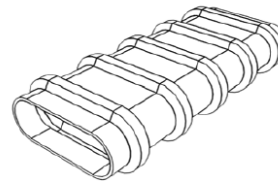
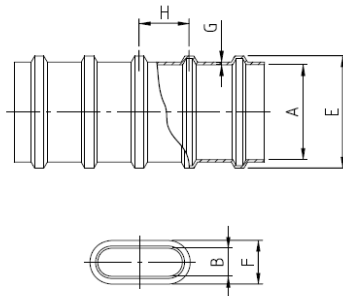
# ANEX I: Specifications for the Flat GDP plastic duct (DYWIDAG)

Table 4: Slip values and locking of wedges

Anchorage or coupler	Slip	Locking measures
—	mm	—
Stressing anchor - Wedge plate - Anchor plate SD - Coupler plate R	3 <sup>1)</sup>	power-seating 20 kN per strand
	6 <sup>1)</sup>	—
Draw-in at stressing anchors to be considered for calculation of elongation	1	—
Fixed anchor - Wedge plate - Anchor plate SD	1	pre-wedging with $P_{0,max}$
	5	—
Bond anchorage	0	—
Fixed coupler R - 2 <sup>nd</sup> construction stage	4	spring
Movable coupler D	8	spring

NOTE

<sup>1)</sup> Slip occurs by transfer of prestressing force from jack to anchorage.



Flat GDP plastic duct			38 × 22	72 × 21	76 × 25	91 × 22
Number of strands $\varnothing$ 15.7 mm			2	3	4	5
Dimensions of cross section						
inside	A	mm	37.5	71.0	75.5	91.0
	B	mm	21.5	21.0	25.0	22.0
ribs	E	mm	52.5	85.5	90.0	105.0
	F	mm	36.5	36.0	40.0	40.0
Wall thickness	G	mm	2.0	2.0	2.0	2.0
Rib distance	H	mm	40.0	40.0	40.0	40.0
Distance of supports		m	0.5			
Wobble coefficient		k	rad/m			
			0.008			
Friction coefficient						
weak axis	$\mu$	rad <sup>-1</sup>	0.12			
strong axis	$\mu$	rad <sup>-1</sup>	0.14	0.15	0.20	0.25

NOTE Dimensions rounded to the closest 0.5 mm.